Experimental setup of the dry test for gyroscopic-pendulum wave energy converter

Zhiyuan Su

Master Thesis

Offshore & Dredging Engineering
September 30th, 2019

TU Delft

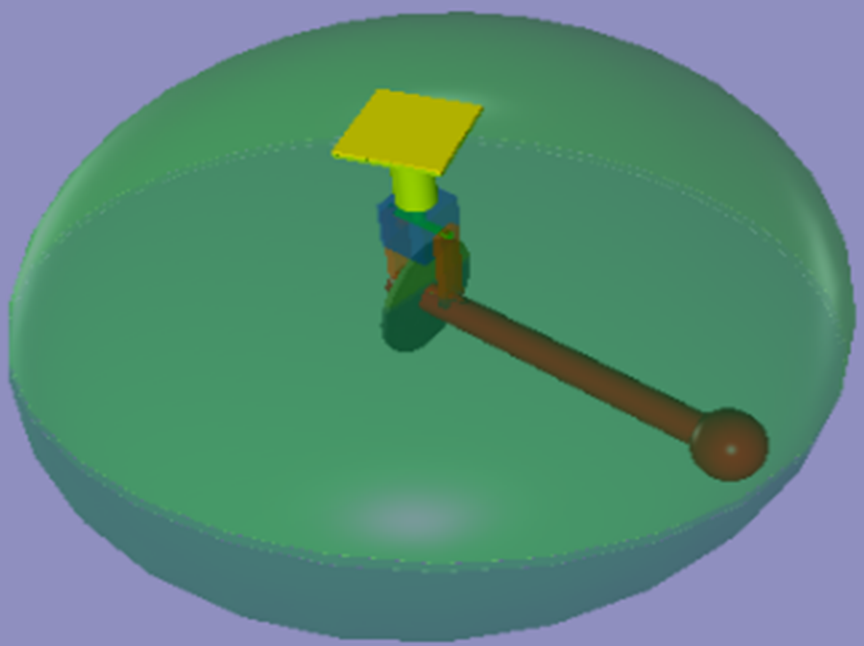

EXPERIMENTAL SETUP OF THE DRY TEST FOR GYROSCOPIC-PENDULUM WAVE ENERGY CONVERTER

Thesis

for the purpose of obtaining the degree of master
at Delft University of Technology,
to be defended publicly on
Monday 30 September 2010 at 13:00 o'clock

by

Zhiyuan SU

from Offshore and Dredging Engineering,
born in JiangSu, China

The chair of the master thesis assessment committee:

Prof. dr. A. Metrikine,	Delft University of Technology

Committee Members:

Prof. dr. A. Metrikine,	Delft University of Technology
Dr. H. Hendrikse,	Delft University of Technology
L. M. Masturi M. Sc,	Delft University of Technology
Dr. F. Pisanó,	Delft University of Technology

PREFACE

Two and a half year ago, I made the decision to come to Delft University of Technology for Master degree. I was just feeling Delft might teach me something which can help find a job. Well that's true. However, when I look back on two-year stay here, the most important thing is this experience makes me realize what life is all about and insist on what you like. Sometimes, life and study are really tough, letting me doubting myself, I would encourage myself "Don't be the one who retreat but rather one who would take up the gauntlet." Two years later, I am so proud I have been here. As I almost finish the thesis, this is my last work as a student, I should admit that coming to Delft is one of the best choice I ever made, it's a really amazing trip coming to Netherlands, studying, living and making connections with a lot of great teachers, friends as my life guider. I really appreciate it.

My thesis topic is interesting and challenging, no one can complete the thesis without help, here I would like to express my greatest gratitude to those who assisted me to accomplish this graduate program.

Great great thanks to Andrei Metrikine, Hayo Hendrikse and Mamin Matsuri as my supervisors for guiding me all along in my thesis, teaching me knowledge and helping me solve the problems. This is my great honor. Hayo is a really reliable guy, giving me a lot of advice on the working direction. Without him, I would get lost in this project. And Mamin is so patient and hard-working, I asked Mamin too many questions, and he gave me the answer one by one, pointing my mistakes and providing his advice. I really really appreciate it.

Thanks for my friends, thanks for your company and support. I am so lucky to meet you guys: Da ge, A shu, Biao Di, Zi Dan, Chen Yue, Yi hui, Mama tian, ZZQ, Shaobin Deng, Wan Huang, Jiaxi Han... Best luck to all of you.

Last but not least, thank you my parents, my grandmother, my whole family, it is my great luck to be same blood with you. Always missing you, my grandfathers and grandma.

Zhiyuan Su
Delft, September 2019

ABSTRACT

Oceans account for 71 percent of the earth's surface, marine resources and energy are abundant. Therefore, making full use of marine energy is a good choice for humans to solve the energy crisis. One way to capture ocean energy is converting wave energy to electrical energy, by means of devices called wave energy converters (WECs).

This project introduces a new type of wave energy converter named "Gyroscopic-Pendulum Wave Energy Converter (GP WEC)". Compared to the classical vertical axis pendulum WEC, a flywheel is added in the system. In combination with the floater motions it creates a gyroscopic effect on the pendulum causing it to rotate, a power take-off device is connected directly to the rotating pendulum shaft in order to harvest the wave energy and generate electrical energy.

To investigate whether this new type of WEC will generate more energy than the classical one, this thesis proposes a dry test setup for the gyroscopic pendulum allowing for systematically investigating the gyroscopic effect on its power output.

This thesis starts from the design of the GP WEC dry experiment and then provides the clear definition of all the components of equipment, along with the applicable scaling laws of all the components and parameters. Also, the requirements as to limits of the equipment are studied with a parameter study.

Using the results of the parameter study a numerical model of the GP WEC is used to simulate the dry-tests. Based on these simulations the range and number of parameters that will be tested in the future experiment are confirmed, and test matrices defined. Some interesting observations from the numerical simulations are further studied looking into the time domain response.

This thesis concludes with the definition of a test setup for dry experiments to be executed at TU Delft in a follow-up study, test matrices for investigating the gyroscopic effect on the power output are defined, and simulation results are presented which can be used for later validation of the physical model.

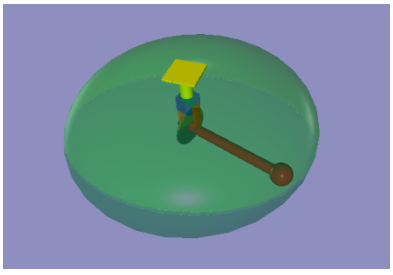

Figure 1: Gyroscopic-pendulum wave energy converter

CONTENTS

1

INTRODUCTION

1.1. BACKGROUND

1.1.1. OCEAN WAVE ENERGY AND WAVE ENERGY CONVERTER

Oceans account for 71% of the earth's surface, while land accounts for only 29%. Marine resources and energy are abundant. Therefore, making full use of marine energy is a good choice for humans to solve the energy crisis. Since more than 100 years ago, human beings have been exploring the huge energy of the vast ocean.

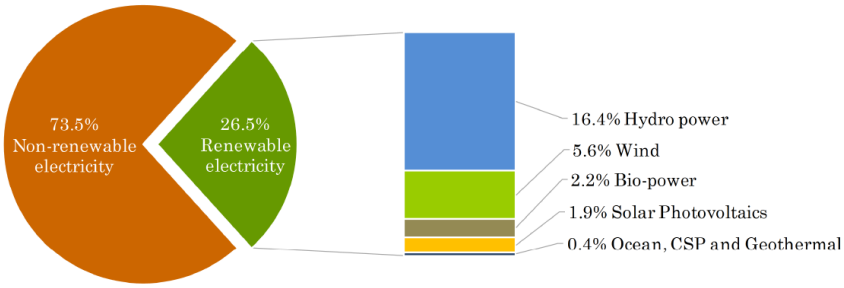

Figure 1.1: Estimated renewable energy share of global electricity production for 2017[1]

Ocean energy usually refers to renewable natural energy in the ocean, mainly tidal energy, wave energy, current energy , sea water temperature energy and sea water salt energy. More broadly, marine energy includes ocean wind energy, ocean surface solar energy and marine bio-energy. According to the storage form, it can be divided into mechanical energy, thermal energy and chemical energy. Among them, tidal energy, ocean current energy, wave energy are mechanical energy, sea water temperature difference energy is thermal energy, sea water salt difference energy is chemical energy. Marine energy is a kind of renewable energy with huge potential[2], clean and pollution-free, but

1

it has the disadvantages of strong regionality and low energy density.
Wave energy plays an important role in marine energy development, and it is also the most likely energy to be widely used [3]. From a technical point of view, it is also the most difficult technology. Waves are unstable and variable in size. If we want to make full use of wave energy, a power generation system must be designed to overcome the different sizes of waves. A more important condition is to have a high rate of return on investment and a high proportion of electricity input per unit, in another word, reducing the levelized cost of energy [4].
Wave energy converter(WEC) refers to the device which can convert wave energy into electrical energy, the principle of it is nothing new.
In recent decades, many researchers made great efforts on the development of different forms of WEC. The patents of WEC have existed since the late 1790s [3], however, modern research on the wave energy conversion started in 1970s by Stephen H. Salter of The University of Edinburgh [5]. He published his WEC called Duck in the Journal of Nature, which is the first Pendulum Wave Energy Converter. After this, from 1990s to nowadays, more research was conducted into the area of wave energy, and thereby more kinds of design on WEC had been published including point absorbers, attenuators, terminators and Oscillating water columns [6] (see Section 2.1). The working principle of the WECS will be discussed in Chapter 2.
However, the most effective way to extract wave energy remains uncertain [7], the current technology of WEC can only extract around 15 percent of the total wave energy all around the word [3], due to the irregular nature of water surface and limit of cost-competition of existing WEC devices. Therefore there is still no widely acceptable design of WEC [7]. To improve the deign of existing WEC on their economic benefits is an important topic for all the researchers.

1.1.2. GYROSCOPIC-PENDULUM WAVE ENERGY CONVERTER

This project introduces a new type of wave energy converter named Gyroscopic-Pendulum Wave Energy Converter(GP WEC). The sketch of this WEC shown in Figure 1.2.

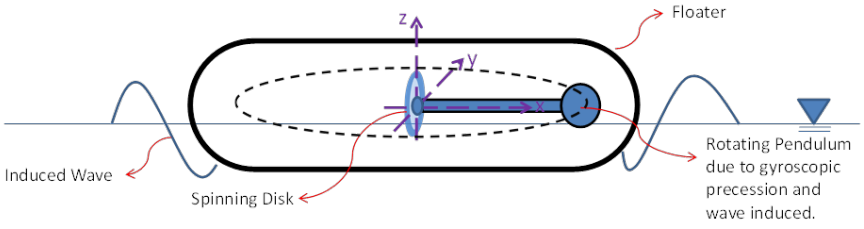

Figure 1.2: Sketch of Gyroscopic-Pendulum Wave Energy Converter

In this figure, we can see a floater as the outer structure for the entire device, moving following the wave. The internal structure is a gyroscopic system, consisting of a spinning disk and a rotating pendulum. This system is located at the centre of rotation and fixed in horizontal direction to the floater. When working in real sea state, wave tilts the floater and induces the pitch motion around the y axis, the spinning disk acts as a

flywheel, combining with the floater motion together and it creates a gyroscopic effect on the pendulum. The rotation of pendulum with a certain moment of inertia will be damped by PTO system which can convert kinetic energy into electricity energy. As mentioned, the gyroscope system has fixed connection to the floater, so the rotation motion of pendulum is directly coupled with the floater motion, in other words, coupled with the hydrodynamic effects on the hull.
The use of gyroscope and pendulum is not brand new for the wave energy converter, the similar working principle used in the VAPWEC and ISWEC is shown in section 2.2. However, for the GP WEC we are studying, it's creative to use pendulum to extract energy in the gyroscope system. In this thesis, it is focused on the dry test design and modelling of the gyroscopic-pendulum system

1.2. SCOPE OF WORK

For the Gyroscopic-Pendulum Wave Energy Converter, Since the numerical model of this device is proposed, (see section 2.4), it is really interesting to us that whether gyroscopic-pendulum system is able to increase the rotation velocity of the pendulum compared to the Vertical Axis Pendulum (VAP), a great and direct way to prove it is conducting dry experiments.
In my thesis, to prepare for the dry tests of experiments, a detailed experimental design and numerical simulation should be done, as well as a detailed test matrix. So for me, the aim of this research is set as:

- **To propose a dry test setup for the gyroscopic pendulum allowing for systematically investigating the gyroscopic effect on its power output.**

Under this aim, the investigation of the system configurations due to the floater motions which can meet the experimental requirements should be presented in the thesis. Considering the full scale device is complicated and not suitable for laboratory tests, its design is also time-consuming, we decide to only perform the scaled down device in the dry environment experiment, in another word, designing motion platform to mimic the hydrodynamic effects. During the design of experiments, an initial test matrix will be given at the end of design in Chapter 3.
After that, in Chapter 4, a numerical model of this system will be provided for modelling of the gyroscopic-pendulum to predict the performance in dry experiment. Firstly, based on the design, some inertial parameters will be input into simulation. Then, a preliminary analysis on the output data will be done to test each parameter on their sensitivity and interactions and their effects on the net energy output, in order to improve the test matrix, making it focus on the parameter combinations we are really interesting in. Then we will change the parameters in the programming and see the performance of the pendulum rotation and energy output. It is intuitive to plot the trend of net energy output as figures in term of different parameters, which is convenient for us to analyze and compare them.
Based on the research goal we have for this thesis project, the scope of work is proposed, which is divided into 4 phases:

1

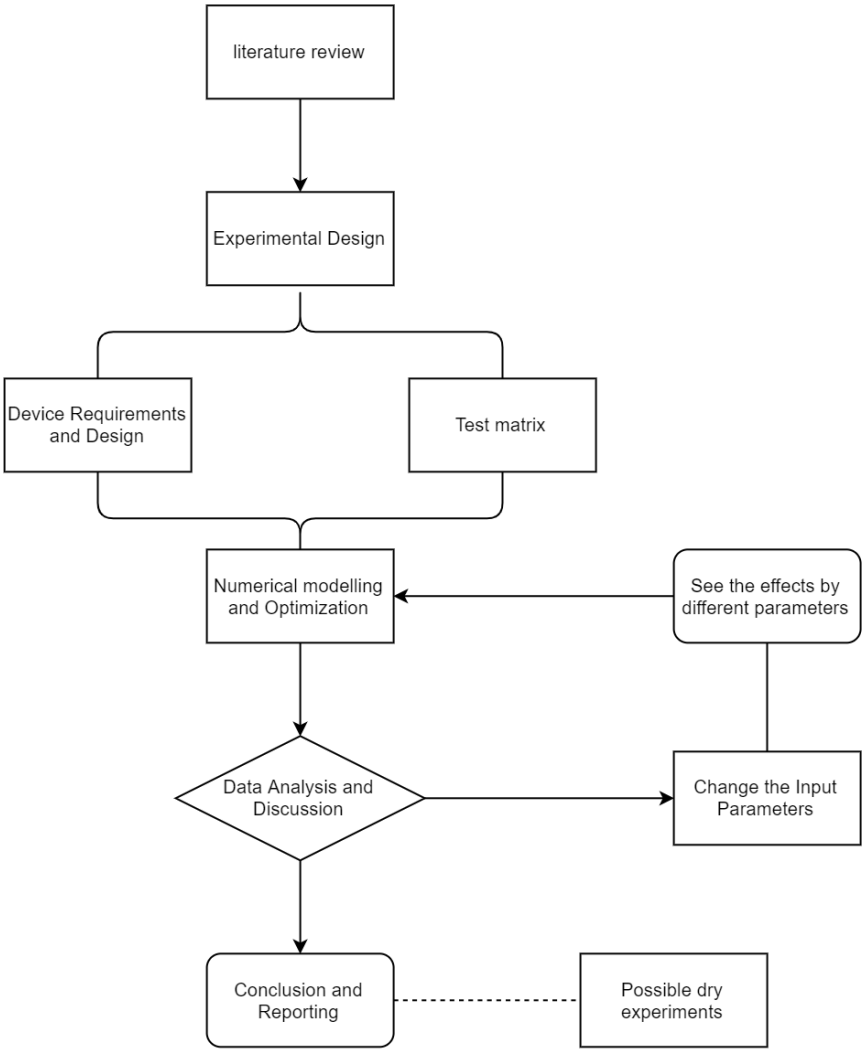

Figure 1.3: Flow chart of research approach

1. Phase 1: Literature review

   (a) Study the design of scaled wave energy converter

   (b) Study the 3D rigid body dynamics

   (c) Study the concepts of numerical model of gyroscopic-pendulum wave energy converter

2. Phase 2: Experimental design

   (a) Study all the parameters

   (b) Define the external force (from the floater motions) with the assumption from numerical model we have

   (c) Define the requirements of experimental equipment

   (d) Define the test matrix and design the test sets

3. Phase 3: Model simulation and optimization

   (a) Choose the suitable motions input

   (b) Find the suitable inertial properties of pendulum and disk

   (c) Do the simulation and preliminary analysis

   (d) Improve the test matrix

   (e) Find the interesting parameters combinations we want for the dry experiments

   (f) Redo the simulation and record the performance of the pendulum.

4. Conclusion and recommendation:

   (a) The design of experimental setup will be concluded

   (b) Recommendation of this research including limitations and further direction

A flow chart of my research approach is shown in Figure 1.3.

1.3. RESEARCH QUESTION

The idea of this thesis project is designing and modelling the dry test experiment in order to investigate the effect of the flywheel coupled with the floater motions to the pendulum rotation. The point of discussion is whether by introducing the flywheel in the gyroscopic-pendulum system able to increase the rotation velocity of the pendulum compared to the pendulum system only. My task during this project includes designing all components of the equipment of experiments and study parameters of experiment, then modelling the dry tests to have an ideal data analysis for experiments. Some advice of improvement on the design and test matrix will also be included.
Therefore, a general research question is addressed from the difficulties in this process:

- **What are the requirements of the GP device and the experimental setup for the dry test?**

To answer this research question, some key problems and how to solve them should be considered during my research, and the approach of my research is shown below:

1. What are the design requirements of the dry test setup? (Including design of the device and test matrix)
   At the beginning of my project, the first question we are facing is the design of all the experiments as no device or prototype are provided for this research. In this case, how to have a clear mind on entire experiments plays an important role, the experimental requirements should be proposed, and some clear and meaningful test matrices should be presented before the conduction of experiments.

2. How the input parameter of the floater motions is implemented into the simulation?
   The motion of floater is directly coupled with the pendulum rotation. How to mimic the hydrodynamic effect on the outer structure is a question, it influences the performance of energy output significantly. The input of motions don't mean it should perform exactly the same irregular wave effects on the platform just like the real sea, it will be too complicated and random, along with uncertain numerical model. Therefore, in this stage, some reasonable assumptions of hydrodynamic effects should be proposed and reasonable motion input should be set. For the numerical modelling, the simplified harmonics in one or two direction will be applied on the system, and we will focus on the the frequency and amplitude of the motion to investigate their effects on the net energy output and the interaction with parameters of gyroscopic pendulum system.

3. Design optimization of the simulation system based on different inertial properties of the pendulum and the flywheel.
   Similarly as the motion input, the input of inertial properties of spinning flywheel and pendulum should be considered carefully as well for their rationality. Not alike with the motion, the different inertial properties work for obtaining the optimum energy conversion efficiency of the device. When we model the gyroscopic pendulum system in programming, it is necessary to consider the real situation in dry experiments, if the range of inertial properties exceeds the capability of motion platform, the meaning of modeling is limited. When considering the inertial properties, it is necessary to cohere, for instance, mass, length of pendulum and mass, radius of disk with each other. One other point which needs discussion is the sensitivity of parameters of system, looking for the parameter which matters most in the system does help the process of experiments a lot.

4. How to simulate and show the performance of pendulum in modelling.
   In this step, the results of modelling have be analyzed to get the conclusion about the parameters' effects on the net energy output, and see how to conclude these effects and optimize the system. The test matrices for dry experiments should also be updated based on these. Under this circumstance, the performance of pendulum and disk with different inertial properties and input motions can be shown and presented in the modelling. Since the energy output can be calculated, the difference of pendulum rotation between different sets of tests is hard to present. We can choose some interesting parameter combination, and show what happen in the system in these cases in order to prepare for the real experiments.

1.4. THESIS OUTLINE

Chapter 1: Background of wave energy, background and basic idea of Gyroscopic-Pendulum Wave Energy Converter.
Chapter 2: Literature review including Wave energy converter, 3-D rigid body dynamic knowledge and some other analysis approaches.
Chapter 3: Experimental design including experimental device requirements, scaling law and test matrix deign.
Chapter 4: The preliminary on parameters, improvement on test matrices based on the analysis.
Chapter 5: Simulation of disk and pendulum's performance by modelling, for the parameter cases studied in Chapter 4.
Chapter 6: Conclusion of the thesis including all the design and analysis, the preparations for the dry experimental setup.
Chapter 7: Recommendation of the research and suggestion for further research and experiments.

2

LITERATURE REVIEW

In this chapter, literature review is done for the basic knowledge of my research. As the aim of my work is to to propose an experimental setup for a dry test of the gyroscopic pendulum wave energy converter, the previous scaled model and experiments focusing on similar area are of great interest. In the first section, the scaled models of Wave energy converters will be studied, it includes both VAPWEC and ISWEC to compare the system with or without the spinning flywheel and see the effects of it. After that, the multi-body dynamics of this system will be analyzed in order to obtain a mathematical model of this system, following the numerical model which is for the data input and experimental validation. At last, analysis method will be proposed for the data analysis and improvements of experimental design.
Although the history of study on wave energy can be traced to the times of Archimedes, it's the decreasing oil reserves and global warming refocused our interest in this research. The recent researches of wave energy conversion date back to 1970's [5], a great deal of work focused on the design of systems for WEC [8], among these researches, people realize that there is huge energy stored on the water surface and the working principle of conventional wave energy converter has been presented.

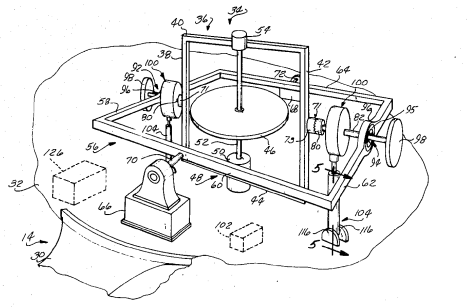

Figure 2.1: Buoyant body with gyro-wave energy transducer [8]

For instance, there exist some patents like references [9] [8] showing various thoughts on how a WEC can be built. Figure 2.1 illustrate a previous work on wave energy conversion by a buoyant body from Herbert K Sachs and George A Sachs's. Although there is no prototype tested in this period, these work inspire people to investigate this topic.
Meanwhile, some work on the analytical solutions of energy conversion and how to optimize the controlling mechanism have been proposed [10] [11]. More researchers realize that converting the energy from random, slow and with high-extreme value into the phase-locked sinusoidal electricity is very hard. In this case, it contains a couple of work on the linear wave energy modeling and creates the foundation for different kinds of WEC design. Starting from the linear wave assumption help simplify the complicated real wave environment and establish the dynamics foundation for the future laboratory tests. Figure 2.2 illustrates the different wave patterns computer simulation without and with energy absorption from Diana Bull and Margaret E Ochs.

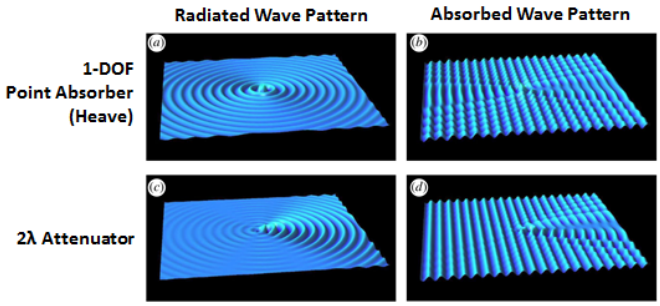

Figure 2.2: Computer simulation of regular wave pattern and energy absorbed wave pattern [12]

The progresses of the computer simulation [3] [12] on this issue in this century brought the advantages to the progresses of a range of different control strategies, and they point out the reason application of wave energy converters not suggested is due to low efficiency, making these kinds of devices losing the advantages of economy. The approach of increasing energy conversion efficiency is developed day by day along with advanced computer modeling and simulation. The continued research and development in the design for harvesting wave energy to increase the efficiency and robustness of the systems has been emphasized more and more [10] [13]. Also some devices have been applicable and commercialized [14].

2.1. WAVE ENERGY CONVERTERS

For the deployment of Wave Energy Converter in site, different physical principle of WEC have been studied and put into operation. Based on different classification rules, the wave energy converters have a lot of categories. According to the position with respect to the wave length, it can be classified into: point aborbers, attenuators and terminators. Accoording to the locations, there are shoreline, nearshore and offshore. They can also be classified by working principle including Oscillating wave surge converter, Oscillating water column, and Submerged pressure differential. The Figure 2.3 illustrates the sketch

of 6 types of WECs' shape. These These typical types of WECs are discussed in this section.

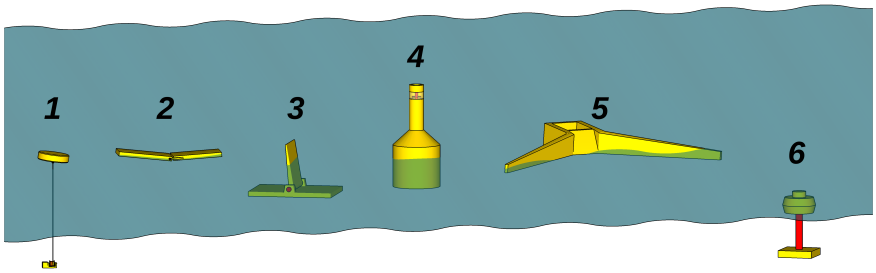

Figure 2.3: Generic wave energy concepts: 1. Point absorber, 2. Attenuator, 3. Oscillating wave surge converter, 4. Oscillating water column, 5. Overtopping device, 6. Submerged pressure differential [15]

2.1.1. POINT ABSORBER BOUYS

A point absorber is the wave energy converter having the horizontal dimension relatively negligible compared with the wave length. It floats on the water surface and is normally connected to the seabed by cables. A point absorber generates energy while rising and falling following the wave. Figure 2.4 shows an example of a point absorber.

Figure 2.4: Ocean Power Technology's PowerBuoy,A point absorber [16]

2.1.2. SURFACE ATTENUATORS

The working principle of attenuators is similar with that of the point absorber, however, it has comparable length to the wave length, whose length parallel to the incoming wave.

This kind of WEC always has a combination of multiple segments connected with each other, example shown in figure 2.5. While attenuator rides on the wave, due to its long dimension, there will exist a relative movement between the segments in order to generate energy.

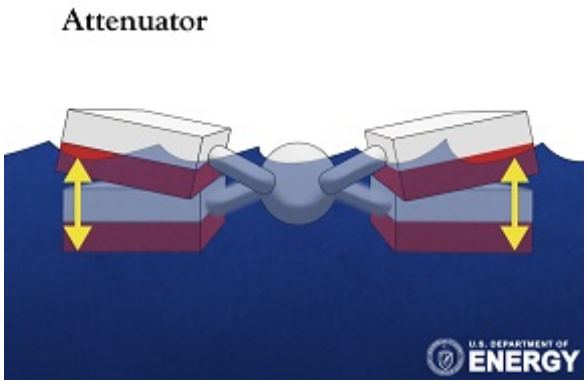

Figure 2.5: Working principle of Attenuator [17]

There is also another WEC called Terminator, whose principal axis lies parallel to the dominant length of a wave crest.

2.1.3. OSCILLATING WATER COLUMNS

Oscillating Water can be located onshore or deeply offshore, fixed onshore or seabed. When the wave moves into the oscillating water column, it will compress the air inside the chambers, creating the pressure difference, and push the air through the turbines to generate energy.

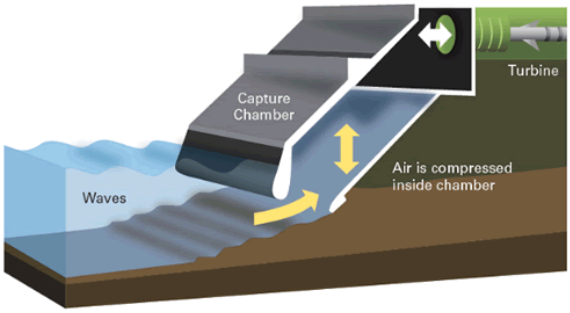

Figure 2.6: Working principle of Oscillating Water Column [17]

However, this device will create huge noise onshore, as the air is pushed through turbines, affecting birds of people living around, If it is located on the seabed, the problem by the chemical or pollution can not be ignored either.

2.1.4. OSCILLATING WAVE SURGE CONVERTER

Provided in figure 2.7, the oscillating wave surge converter has an one end fixed on some kind of structure or just on the seabed. It extracts energy by the relative motion of the flexible body following with the wave motion, since it swings forth and back compared to the fixed point on the seabed.

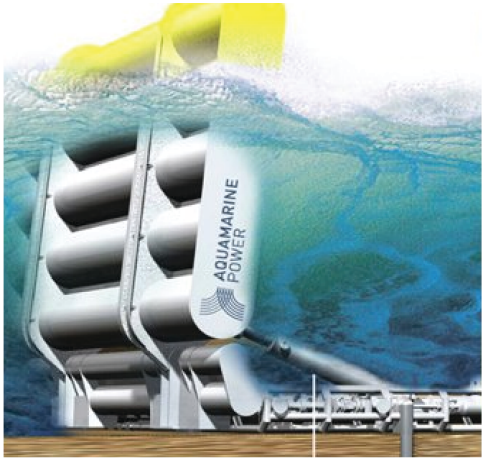

Figure 2.7: Example of an oscillating wave surge converter, Aquamarine Power Oyster [18]

2.1.5. SUBMERGED PRESSURE DIFFERENTIAL

Similarly with the oscillating wave surge converter, the submerged pressure differential is also fixed on the seabed and submerged. The working principle of this kind of WEC, however, is just like its name, it depends on the pressure changes at the position of device, beneath the water surface. The device called Archimedes Wave Swing shown in figure 2.8, it uses a semi-heaving buoy just like the point absorber, but to create the pressure differential as propagation of the wave.

Figure 2.8: Example of a submerged pressure differential wave energy converter, Archimedes Wave Swing [19]

2.1.6. OVERTOPPING DEVICE

The overtopping device shown in figure 2.9 is always a long structure, facing the progressing wave. It uses the wave velocity to fulfill a reservoir to store the potential energy, and the potential energy is converted into electricity energy by the low-head turbine besides.

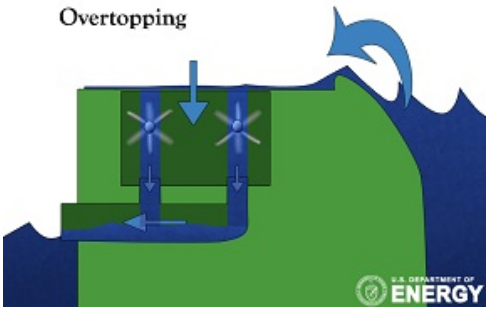

Figure 2.9: Overtopping device [17]

2.2. SCALED WAVE ENERGY CONVERTER

Along with the development of theoretical aspect of wave energy conversion, it is obvious that there will be significant value in building small scale prototype and placing the environment modeling the real sea wave.

Figure 2.10: The Edinburgh curved wave tank

This type of work is more realistic and has more empirical data for future development

of design. The simulation real sea environment help us quickly define the physical phenomenon and validate the efficiency of this technology, which is the advantage over the pure computer modeling analysis.
In recent years, the existence of some wave simulation tank satisfy the deployment and tests of scaled device, the Edinburgh cured wave tank is a good example shown in Figure 2.10. This curved wave tank was constructed in the University of Edinburgh [20]and can generate the simulation wave scaled 1/100 compared with North-East Atlantic waves. This kind of experimental facility contribute to the scaled device which can give accurate response in specific wave conditions. Also, future study of this project can be conducted in wave tank in TU Delft.

2.2.1. VAPWEC

The VAPWEC is abbreviated to Vertical Axis Pendulum Wave Energy Converter which is a point absorber taking off power based on the pendulum motions. The basic opreational concept is shown in Figure 2.11 which is the first VAPWEC patent by Thiokol Chemical Corporation in 1966.

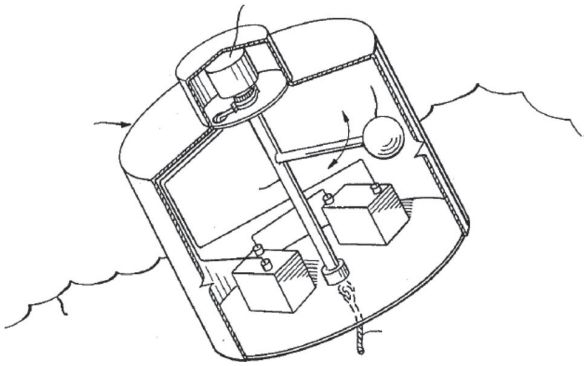

Figure 2.11: Basic operation of a VAPWEC. Patented in 1966 by the Thiokol chemical corporation [9],patent number 3231749.

In Figure 2.11, we can see that the axis of pendulum rotation keeps parallel to the body-fixed vertical axis of the Wave Energy Converter, i.e., the VAPWEC is nothing more than an axle-pendulum-bearing assembly connected to a generator [21]. This device generates energy directly by producing tilting moments about the center of gravity by following the wave. It is a typically conventional wave energy converter: without flywheel and recognized as no energy input from device itself, only generating the energy by the coupled motion of pendulum which is connected to the generator. Also, it can produce electricity in any kind of irregular wave. For my research, VAPWEC is also part of research and worth discussion, as comparison with the conventional wave Energy Converter is the critical approach to investigate the effects of flywheel.
Coming to 21st century, a VAPWEC prototype called Vincent created by B.Boren from Oregon State University is really representative and illuminating for us. Boren did a deep research into the VAPWEC from modeling to experiments shown in [22] [4] [21] during his master and PhD. The design of Vincent really inspires us and a CAD model of its de-

sign is provided in Figure2.12.

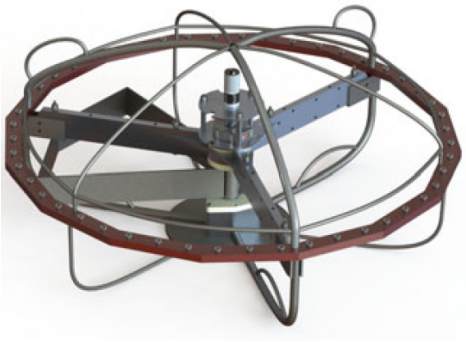

Figure 2.12: Model of Vincent by B.Boren [21]

No matter what kind of design the VAPWEC is, it can be classified as an inertial mass based point absorber WEC [4], converting the energy of the motions of a large inertial mass into electricity. There will be strictly requirements on the material choices and frame design. Furthermore, a suitable power take-off device is also required, since apply a damping torque on the rotation mass is necessary for testing the energy conversion in various conditions of motions.
While this prototype Vincent here is very clear and simplified, only containing the fundamental components including the external and internal structure and some measurement equipment, which provides a suitable reference for design and fabrication. This device was proved reliable while being tested at O.H. Hinsdale Wave Research Laboratory, whose functions are shown in References [23], and this test investigated the general performance of a VAPWEC in irregular waves. The specific analysis of components will be provided in Section 3.3.
Upon the data analysis, B.Boren output the mean net power of device at various wave conditions, and compared the effects of lighter of heavier pendulums, which are all the topics that can be included in this research. When applying the torque on the rotation of VAPWEC, the electrical energy output is directly coupled to the torque, which can be calculated by Equation 2.1

$$\| \vec{P} \| = \vec{M}_t \vec{\omega} \tag{2.1}$$

Where The $\vec{M}_t$ is the various torque applied on the rotation pendulum, and the $\vec{\omega}$ is the rotational velocity of pendulum. Obviously, the applied torque should be on the opposite angular direction with the rotational velocity:

$$\mp \vec{M}_t = \pm \vec{\omega} \tag{2.2}$$

The input torsional force should be defined by Coulomb force theoretically, but the Coulomb force is a nonlinear phenomenon, which is hard for controlling. So to be simplified, the torque is approximated to linear function provided in Equation 2.3 [24] [25].

$$\vec{M}_t \approx -C_N \vec{\omega} \tag{2.3}$$

Where $-C_N$ is the damping coefficient for approximating the applied torsional force.

2.2.2. ISWEC

ISWEC is referred to Inertial Sea Wave Energy Converter, which is a floating device converting the wave energy by rotation motion riding on the wave. Is is also a point absorber as the VAPWEC, moored loosely to the seabed [26] [27]. The gyroscope inside the hull of device will be driven to rotate by some kinds of motor, and the pitch motion of floater will be transmitted into the gyroscope, generating the gyroscopic effect on the main axis. Similarly, the rotation will be damped in order to convert the kinetic energy into electricity, what makes it different is, for the ISWEC, there is energy input into the gyroscope while there is no input into VAPWEC. Also, there is one more axis of roation by ISWEC.
At first, early 20th century, the gyro was introduced in the ship system for damping the roll and pitch motion shown in Figure 2.13. The huge machine was installed in the vessel and produced the gyroscopic effect on the vessel, reducing the roll motion of it to have a stable ride on wave and give comfort to the passengers. It connected to a electrical motor and can be easily turned on or off. The installation of it was quite a miracle for people at that time, also threw a bomb into the ship industry [28].

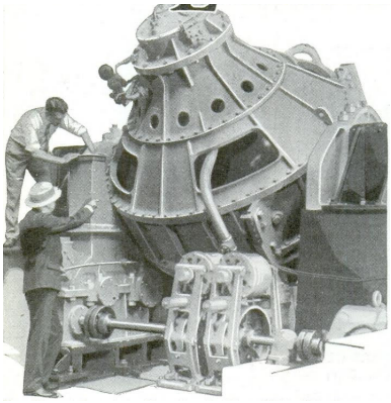

Figure 2.13: Gyro stabilizer in 1931 [28] From Popular Mechanics Magazine

However, for the use of gyro system in extraction of Wave Energy, it started later. In 1982, Herbert K. Sachs [8] shows the gyro in the WEC system to extract energy from wave by coupling it to the hull and an electrical generator, its sketch provided in Figure 2.1.Although this design of gyro-Wec is limited by its applicability, it already had all the fundamental components for conduction in wave. A gyroscope is mounted in the internal frame, its rotation axis is perpendicular to the rotation of external frame. A motor is connected to the gyroscope for controlling the rotational velocity, along with a generator producing a damping torque on the rotation for converting kinetic energy to electrical energy. A full dynamic and controlling system was shown in Reference [8]
Coming to the recent research, the work by Giovanni Bracco from Politecnico di Torino in recent 10 years derives deeply into ISWEC from the numerical model to the prototype design, including scaled 1DOF and 2DOF device, along with the full scale prototype. In Figure 2.14, it illustrates the CAD drawing of 1 DOF ISWEC prototype [29] [30]. When the

wave comes into the ISWEC, it rocks the floater, generating the pitch motion δ, and this motion will be transmitted into the gyroscope system carried inside the device. The gyroscope acts as a flywheel and produces a spinning velocity $\dot{\varphi}$, the combination of these two motions creates the gyroscopic effect on the PTO axis, inducing the rotation ε. This rotation will be used for damping and generating electricity.

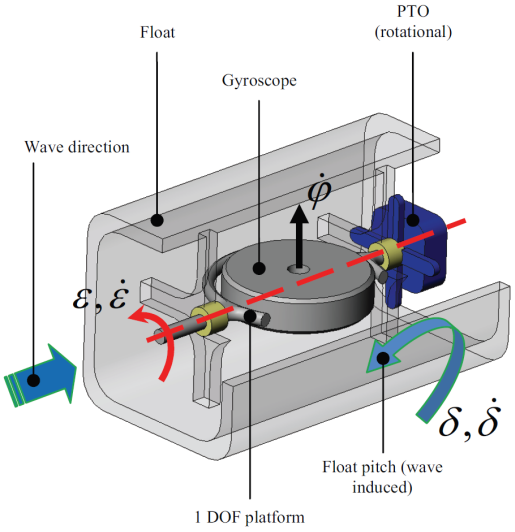

Figure 2.14: 1DOF ISWEC by Bracco [29]

For a specific design, the equation of motion of gyroscope system is shown in Equation 2.4 around the PTO rotational axis.

$$I\ddot{\varepsilon} - J\dot{\varphi}\dot{\delta}\cdot\cos\varepsilon + (I-J)\dot{\delta}^2 sin\varepsilon\cdot\cos\varepsilon = T_\varepsilon \tag{2.4}$$

Where J is the moment of inertia of the flywheel around its spinning axis, and I represents the moments of inertia of flywheel around other two axes.
However, for simplification and linearization, Bracco [29] [30] assumed

1. The device is designed with I≃J,
2. The gyroscope has a constant spinning velocity.
3. The angle ε is linearized the angle $\varepsilon = 0$

Under these assumptions, the equation of motion 2.5 describes a linear gyroscopic system, in which giving a input δ and observing the output ε

$$J\ddot{\varepsilon} + c\dot{\varepsilon} + k\varepsilon = J\dot{\varphi}\dot{\delta} \tag{2.5}$$

The output angle cannot be sufficient for the research, the extracted energy at the resonating conditions ($\omega = \omega_n$) was calculated by Bracco with Equation 2.6

$$P_d = \frac{J\dot{\varphi}\omega\delta}{2c} \tag{2.6}$$

Substitute the damping coefficient c with the working principle of the PTO, Equation 2.7 is obtained.

$$P_d = \frac{J\dot{\varphi}\omega\delta}{2\frac{2P_d}{\omega^2\varepsilon_0^2}} = \frac{1}{2}J\dot{\varphi}\omega^2\delta_0\varepsilon_0 \tag{2.7}$$

From Equation 2.7, we can see, to extract more energy from the PTO, except increasing the moment of inertia, rotational velocity of each axis, a short period wave is also helpful for the energy extraction of device [30] [29].
After the design of this device, the 1DOF prototype was fabricated in a scale as 1:8 for both dry test and wave tank test using facilities of the Universities of Edinburgh and Naples [31]. For the dry test, two different types of wave simulation rigs which can provide pitch motion was used shown in Figure 2.15 [32] [30].

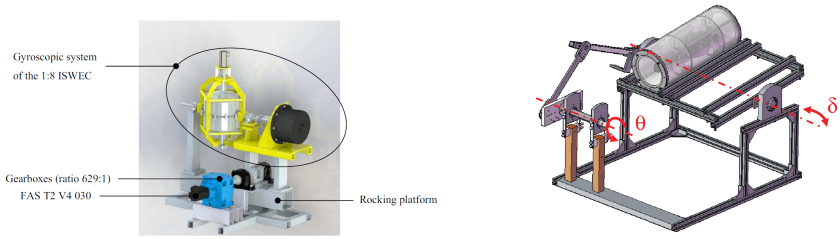

Figure 2.15: Two different kinds of motion platform

Two simulation rigs have different aims, the left one is designed for the Hardware-In-the-Loop test [32], while the right side one exists for the extracted energy test. However, the both of simulation rigs provide the reference on the design and controlling strategies, the motion platform we will use must include the fundamental components just like them. Additionally, only pitch motion doesn't satisfy our research, more motion combination should be provided on our gyroscopic system, it will be explained in Section 3.1.
The 2DOF scaled prototype and full scale prototype were also studied by Bracco in Reference [29] [21] [33] [34].

2.3. DYNAMICS

This section discusses the dynamics system for the gyroscopic-pendulum wave energy converter, mainly about the 3D rigid body dynamics or multi-body dynamics. The Euler angle of the 3D rigid body dynamics will also be emphasized in this part. As there is no standard notation for Euler angles, a typically used one was applied shown in Figure 2.16.
It shows Translation:

1. Surge is translations in x – direction
2. Sway is translation in y – direction
3. Heave is translation in z – direction

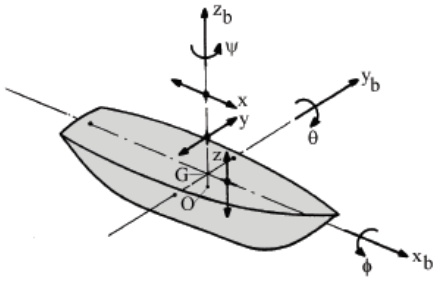

Figure 2.16: Six Degrees of freedom motions

Rotation:

1. Roll (ϕ) is rotation about x_b – axis
2. Pitch (θ) is rotation about y_b – axis
3. Yaw (ψ) is rotation about z_b – axis

But to analyze the angular velocity and angular orientation of the rotating body, a reference system attached to the body is necessary to describe, then the position and velocity of all the components on this body can be described.

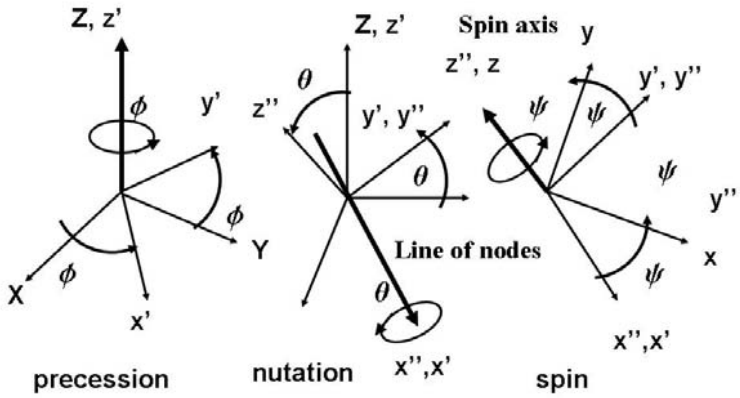

Figure 2.17: Euler angle: precession, nutation, spin

Figure2.17 shows how the body-fixed coordinates (x, y, z) rotates with respect to the fixed

coordinate(X,Y,Z). The motions of three-dimensional rigid body can be described by these translations of the coordinates, which are also called the Euler angles. As shown, the axis can precess through an angle ϕ, nutate through an angle θ, and spin through an angle ψ.
To have the equation of motion of this 3D rigid body system, firstly, in the left of Figure 2.17, we rotate the coordinate around the$Z$ axis firstly, so Z axis remains still, while X, Y rotate an angle ϕ but keeping in the X, Y plane, resulting in the the coordinate (x', y', z'). This angle ϕ is called the angle of precession illustrated in Equation 2.8, which is also the rotation of pendulum in our system. In this equation, it also shows the transformation matrix can be simplified into $[T_1]$.

$$\begin{bmatrix} x' \\ y' \\ z' \end{bmatrix} = \begin{bmatrix} cos\psi & sin\psi & 0 \\ -sin\psi & cos\psi & 0 \\ 0 & 0 & 1 \end{bmatrix} \begin{bmatrix} X \\ Y \\ Z \end{bmatrix} = [T_1] \begin{bmatrix} X \\ Y \\ Z \end{bmatrix} \tag{2.8}$$

After that, this system rotates through the y' axis, which is also the rotation of pitch in our system, the axis of rotation for this is called the "line of nodes". The x', z' axis rotates an angle θ while y' remains still, leading to a coordinate (x'', y'', z''). This angle is called the angle of nutation.

$$\begin{bmatrix} x'' \\ y'' \\ z'' \end{bmatrix} = \begin{bmatrix} cos\theta & 0 & -sin\theta \\ 0 & 1 & 0 \\ sin\theta & 0 & cos\theta \end{bmatrix} \begin{bmatrix} x' \\ y' \\ z' \end{bmatrix} = [T_2] \begin{bmatrix} x' \\ y' \\ z' \end{bmatrix} \tag{2.9}$$

At last, (x'', y'', z'') spins around x" axis, which is also the rotation of roll in our system, and creates the coordinate (x, y, z). The angle ψ is called angle of spin.

$$\begin{bmatrix} x \\ y \\ z \end{bmatrix} = \begin{bmatrix} 1 & 0 & 0 \\ 0 & cos\phi & sin\phi \\ 0 & -sin\phi & cos\phi \end{bmatrix} \begin{bmatrix} x'' \\ y'' \\ z'' \end{bmatrix} = [T_3] \begin{bmatrix} x'' \\ y'' \\ z'' \end{bmatrix} \tag{2.10}$$

The final Euler transformation is shown in Equation 2.11, it illustrates the combined equation of motion from three Euler angles, as three different translations, which can be regarded as basic translation of body-fixed coordinate.

$$\begin{aligned} \begin{bmatrix} x \\ y \\ z \end{bmatrix} &= [T_1][T_2][T_3] \begin{bmatrix} X \\ Y \\ Z \end{bmatrix} \\ &= \begin{bmatrix} cos\psi cos\theta & -sin\psi cos\theta & sin\theta \\ sin\psi cos\phi + sin\theta sin\phi cos\psi & cos\psi cos\phi - sin\psi sin\phi sin\theta & -cos\theta sin\phi \\ sin\phi sin\psi - cos\psi sin\theta cos\phi & cos\psi sin\phi + sin\psi sin\theta cos\phi & cos\theta cos\phi \end{bmatrix} \begin{bmatrix} X \\ Y \\ Z \end{bmatrix} \end{aligned} \tag{2.11}$$

To calculate the angular velocity, the individual rotation velocity $\dot{\psi}$, $\dot{\phi}$ and $\dot{\theta}$ can be easily obtained from the translation above, but these three angular velocities are expressed in different coordinate, which are z axis, Z axis and x' axis. Therefore, it is necessary to convert the angular velocity into the last coordinate (x, y, z).to calculate ω_x, ω_y and ω_z. In Figure 2.18, it shows how to convert the angular velocity into the same coordinate with

three Euler angles. The specific expression of angular velocities is shown in Equation 2.12. One thing worth mentioning is that the Equation 2.11 only shows the first step of rotation in our system, the effects of spinning should also be considered the same way as the calculations above, which is also included in Equation 2.12.

$$\begin{aligned}\omega_x &= \dot{\phi_d} + \dot{\theta} sin\psi + \dot{\phi} cos\psi cos\theta \\ \omega_y &= \dot{\psi} sin\phi_d + \dot{\theta} cos\phi_d cos\psi cos\theta + \dot{\theta} sin\phi_d sin\theta \\ \omega_z &= \dot{\psi} cos\phi_d - \dot{\theta} sin\phi_d cos\psi + \dot{\theta} sin\phi_d sin\psi cos\theta + \dot{\phi} cos\phi_d sin\theta\end{aligned} \tag{2.12}$$

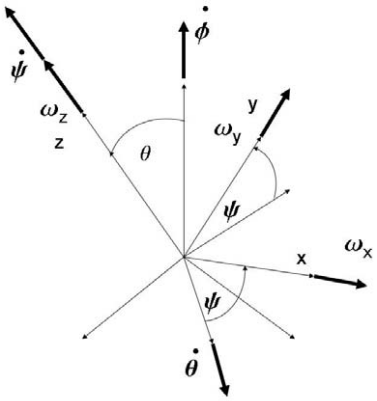

Figure 2.18: angular velocity of 3D rigid system

2.4. EQUATIONS OF MOTION

For the modelling of gyroscopic-pendulum system, a python modeling is provided considering all the parameters on the time domain. To establish the model mathematically, Lagrangian Formulation is chosen as the method to couple the roll and pitch motion of floater with the two motions of pendulum system (disk and pendulum rotation) [35].
The application of Lagrangian Formulation requires calculating kinetic energy and potential energy from all the components in the system. In the gyroscopic-pendulum system, only disk and pendulum produce energy. For the disk, it always locates at the center of system, as well as the origin of local coordinate, so it only contributes kinetic energy (T_d). While the pendulum produces kinetic energy (T_P) from translation and rotation, as well as potential energy from pendulum vertical displacement with respect to the origin of local coordinate. This displacement can be calculated by projecting the pendulum positioning vector on Z_0 ($\vec{r_p}$, $\vec{k}$) where $\vec{r_p}$ is pendulum position vector, $\vec{k}$ is the unit vector of local z axis.

Besides, the potential energy from the restoring force is modelled as the spring on pitch rotation, with stiffness coefficient = k_θ.
The disk kinetic energy is calculated in Equation 2.13:

$$T_d = \frac{1}{2}\vec{\omega_d}^T I_d \vec{\omega_d} \tag{2.13}$$

Where $\vec{\omega_d}$ is the disk angular velocity vector, I_d is the moment of inertia of disk The pendulum kinetic energy is calculated in Equation 2.14:

$$T_p = \frac{1}{2}\vec{\omega_p}^T I_p \vec{\omega_p} + \frac{1}{2}\dot{\vec{r_p}}^T m_p \dot{\vec{r_p}} \tag{2.14}$$

Where $\vec{\omega_p}$ is the pendulum angular velocity vector, $\vec{r_p}$ is the pendulum positioning vector I_p is the moment of inertia of pendulum.
The potential energy can be calculated in Equation 2.15:

$$V = m_p g(\vec{r_p}, \vec{k}) + \frac{1}{2}k_\theta \theta^2 \tag{2.15}$$

Where θ is floater pitch motion, g is the gravitational acceleration.
Based on the energy calculation, Lagrangian Formulation can be obtained below:

$$L = T - V \tag{2.16}$$

$$\frac{d}{dt}\left(\frac{\partial L}{\partial \dot{q_j}}\right) - \left(\frac{\partial L}{\partial q_j}\right) + \frac{\partial F}{\partial \dot{q_j}} = 0 \tag{2.17}$$

Subscript 'j' is the number of degrees of freedom of the system, in this case, j = 4 which means 4 DOFs system including floater roll, pitch, disk and pendulum, along with 4 equations of motion in total. q_j d $\dot{q_j}$ indicate the position and time derivative of the position.
The damping component is introduced in Equation 2.18:

$$F = \sum_j \frac{1}{2} c_j \dot{q_j}^2 \tag{2.18}$$

Where c_j is damping coefficient.
From this process, four equations of motion are obtained for the establishment of python modelling.

2.5. BUCKINGHAM π THEOREM

Buckingham π theorem is a useful method in dimensional analysis for engineering, applied mathematics and physics. Generally, this method proposes that if an physically meaningful equation involves a certain number n physical variables, and these variable can be expressed in terms of independent physical units, then this equation can be rewritten in terms of a set of $p = n - k$ dimensionless parameters π_1, π_2 ... π_p constructed from the original variables.
This method was first proved by French mathematician Joseph Bertrand [36], however,

his considerations only contained some special cases and basic idea of this theorem. The use of this method in a general situation is provided by Rayleigh, about the dependence of pressure drop in a pipe with the governing parameters [37]. Basically, the Buckingham π theorem is a method which help us create sets of dimensionless parameters from given variables even we have not known the equations and relationship of variables. However, this method only helps us build the dimensionless parameters but will not help us find out the physical meaning of it. On the other hand, choosing of dimensionless parameters in this method is also not unique, which means, for the experiments, we should choose the ones which is convenient and may be physically significant for us.
Mathematically, the number of dimensionless terms can be set as p, which is also the nullity of the dimensional matrix, and k is the rank.
Therefore, if we have an equation of a physical system, like Equation 2.19:

$$f(q_1, q_2 ... q_n) = 0 \tag{2.19}$$

where there are n physical variables q_i in this physical equation, and these variable have k independent fundamental units. In this case, this equation can be expressed into Equation 2.20.

$$F(\pi_1, \pi_2 ... \pi_n) = 0 \tag{2.20}$$

Where there are $p = n - k$ dimensionless parameters formed by the original variables q_1, $q_2 ... q_n$, which are called pi groups in the form of Equation 2.21.

$$pi_i = q_1^{a_1} q_2^{a_2} ... q_n^{a_n} \tag{2.21}$$

Where the exponents a_i are rational numbers. We can take the the relationship between drag coefficient C_D and Reynolds number R_e as an example to show how to create the dimensionless π groups. This function between this two parameters shows the phenomenon that the flow goes past a sphere.

1. Choose variables or parameters which may affect the experimental results:
   This is a challenging part, since at the beginning, it's hard to tell which parameters have the effects on other parameters.
   In this system, to study this phenomenon, we intend to measure drag force F, and the parameters may affect it include fluid velocity v, viscosity of fluid μ, density of fluid ρ, and the diameter of sphere D. So there are n = 5 different variables in this system.

2. Count the number of independent units and π groups:
   In this system, we have k=3 dimensions, which are mass(M), length(L) and time(T), so we will have $p = n - k = 2$ π groups.

3. Choose "repeating" variables:
   In this step, we choose the same number repeating variables as the independent variables, which can be D, v and ρ. As the F is the one we want to focus on, so we cannot choose that one as repeating variable.

4. Form the π terms:
   As we have two parameters left excluding repeating variables, we should include them in the equations shown below, combined with the repeating variables:

$$\begin{aligned} \pi_1 &= \mu D^a v^b \rho^c = M^0 L^0 T^0 \\ \pi_2 &= F D^a v^b \rho^c = M^0 L^0 T^0 \end{aligned} \tag{2.22}$$

   In these two π groups, we only need to solve the a, b and c to make them dimensionless,so these two π groups are formed as below

$$\begin{aligned} \pi_1 &= \mu D^{-1} v^{-1} \rho^{-1} \\ \pi_2 &= F D^{-2} v^{-2} \rho^{-1} \end{aligned} \tag{2.23}$$

   From this equation, $\frac{1}{\pi_1}$ is Reynolds number and D^2 can be translated into $\frac{\pi}{4}A$, then pi_2 can be transferred into Equation 2.24, which is so-called drag coefficient.

$$\pi_2 = \frac{F}{(\frac{\pi}{4}A)\, v^2 \rho} \tag{2.24}$$

   In this case, we can see that the parameters themselves are not our focus, we only need to care the dimensions. Therefore, we can change the formation of parameters for our convenience or make it physically meaningful.

As we have two π groups: drag coefficient and Reynolds number respectively, we can test all the parameters in our experiments. Each test having 5 parameters can be translated into two π values, and after repeating this step, a scatter graph of drag coefficient and Reynolds number can be shown in Figure 2.19.
In this figure, we can see that, if the Reynolds number of fluid can be determined, then the its drag coefficient can also be found. In this case, the drag force F can be calculated in this way. The method can help do the experimental analysis.

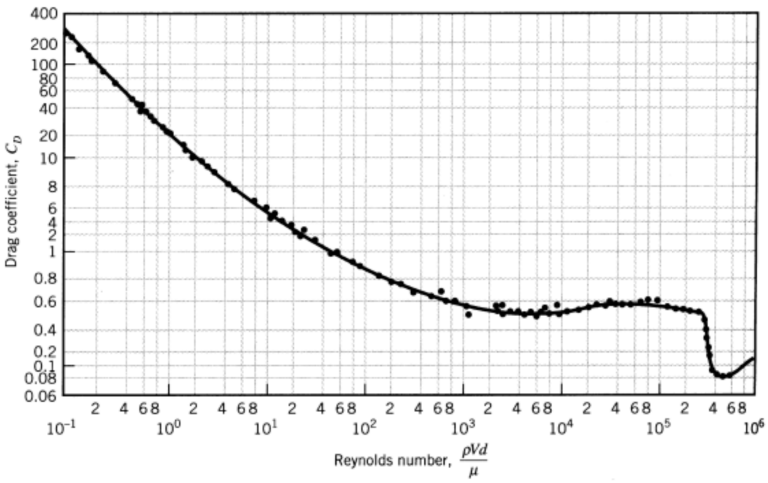

Figure 2.19: The drag coefficient as a function of the Reynolds number

3

EXPERIMENTAL DESIGN

The design of experiments is an important part of this research including the experimental design and test matrix design. At the beginning of this project, the device which will be used was undefined. Therefore, the requirements for the device and the scaling of experiments should be decided to define the dimensions of the experimental equipment. A prototype of wave energy converter will be chosen for the reference of dimension based on suitable scaling law. However, these regulation of device are elastic, since they are only on the theoretical aspect and supported by the previous similar experiments, the specific condition can be different in a certain extent.
At last, a preliminary test matrix should be proposed to have a clear idea on the experimental layout. The test matrix proposed in this section is rough without specific number. An improvement on it will be done in next chapter.
Based on the literature review of scaled wave energy converter, as the dry tests have been applied to my research, some equipment are required to mimic the hydrodynamic effects on the pendulum rotation which is coupled to the motions. The main components include:

1. A motion platform;
2. Gyroscopic-pendulum system consisting of spinning disk (with motor) and pendulum;
3. Measurement equipment (sensor, camera and data data acquisition device etc.)

To dive deeper in to the requirements of device, one begins with dividing the main components into a couple of parameters and studying the requirements.

3.1. PARAMETER STUDY

For the parameters study, the parameters can be classified into the ones we can manage (arguments) and the ones we test (dependent variable) The arguments include the platform motions, spinning disk parameters (moment of inertia, spinning velocity and

position of disk) and pendulum moment of inertia. The dependent variables include the pendulum rotation velocity or energy output. As we want to optimize the pendulum rotation velocity, it's important to require the device equipped with a flexible controlling system.

1. Parameters we can manage

   (a) Floater Motions
   The motions which would be provided by the motion platform is the most important and tricky parameter we have. On the one hand, the advantage of dry test is, if conditions permit, we can have any combination of motions, but on the other hand, the motion combination should be reasonable based on the experimental assumptions, it is unnecessary to perform the motion combination which is meaningless. To decide the reasonable motion combinations for experiments, our thoughts are shown in Figure 3.1. We start from the real sea state, and translate the hydrodynamic effects of real sea state directly into applied motions of platform. However, the real sea state is too complicated, some assumptions of hydrodynamic effects are required for simplification based on the working principle of the ISWEC and several motion combinations would be presented. Afterwards, when the equipment is installed, specific input data would be determined and the experiments would be conducted.

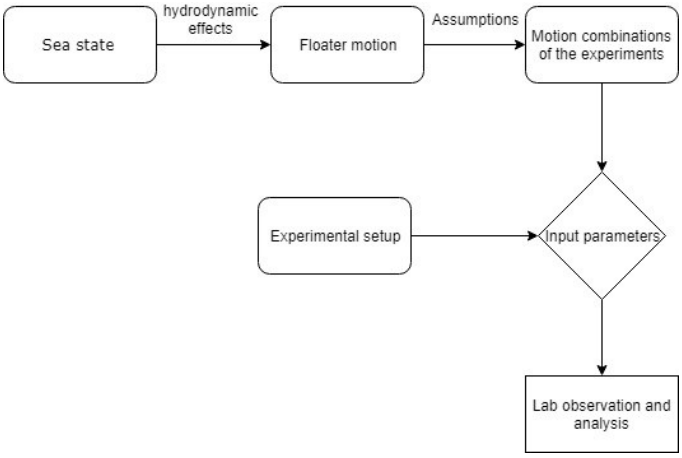

Figure 3.1: Thoughts of the motions input

To understand how the floater motions are in the sea state, Figure 3.2 from Boren's work is shown below. In this figure, four states at four instances of time of WEC are illustrated, subjected to a progressive monochromatic wave. The swinging pendulum is represented as blue and red rectangles. The green dots fixed on the fore of the floater means the heading of the floater keeps the same direction with the progressive wave, which means the yaw and roll are constrained.

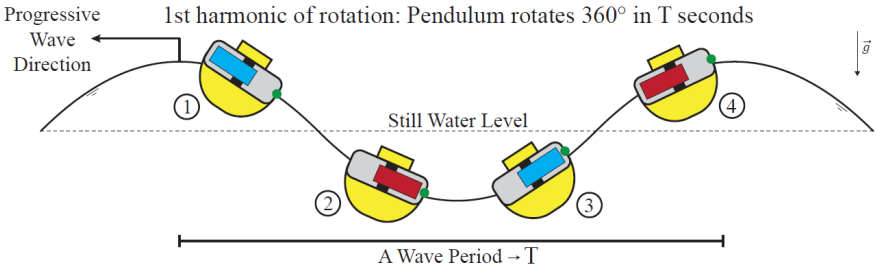

Figure 3.2: Ideal positional states for pendulum relative to a wave crests and troughs [4]

In this special case, the mass of the pendulum effects the hull's orientation in a negligible way. The state 1 and 3 with blue colour represent the pendulum with maximum potential energy, while the state 2 and 4 with red colour show the pendulum with minimum potential energy. In another word, the potential energy of the pendulum corresponds to the rests and troughs of wave profile directly, which means, in this case, this device has the highest energy efficiency. However, a phase shift always exists in reality, decreasing the efficiency [4].
In this condition, the WEC is a 3 DOF-system including pitch, heave and rotation of pendulum. And it is considered as the most simplified condition, any other more complicated assumptions are all based on this initial one. The other combination considered are listed below.

i. If we still assume that the mass of pendulum is negligible, but the bow of the floater does not follow the wave profile perfectly (Only yaw motion constrained). In this case, it can be seen as there exist two wave profiles with different progressive directions. Therefore, the combination of motions in this situation is pitch, roll, heave and rotation of pendulum.

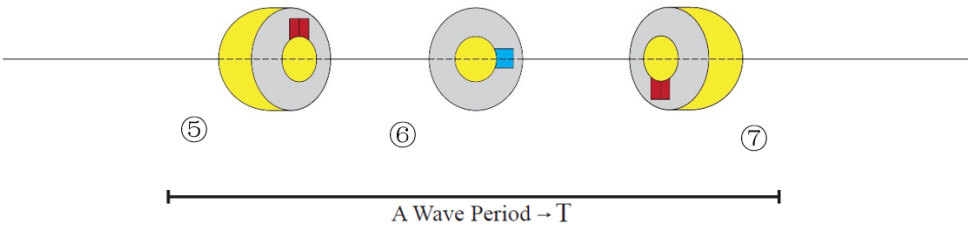

Figure 3.3: Ideal intermediate positional states for pendulum at the top view (the pendulum rotates counter-clock wise direction)

ii. If we assume that the mass of pendulum is not negligible, in which case, the coupling motion of pendulum can influence the motions of floater, and there is only one progressive monochromatic wave. Under this circumstance, illustrated in Figure 3.3, the state 5, 6, 7 are the intermediate states of state 1 and 2, 2 and 3, 3 and 4 at a top view, respectively. When the floater follows the wave from the state 1 to state 2, the pendulum would rotate from the bow to the one side of the floater and the stern finally, which is shown by state 5. During this process, the centrifugal force by the pendulum would drag the whole device and leads to the translation movement.
Under this assumption, the combination of motions is pitch, surge, sway, heave and rotation of the pendulum.

iii. If we combine these two assumptions together that: the mass of pendulum cannot be negligible and the floater is subjected to multiple wave profiles, only the yaw motion is constrained. Based on the concept above, the motion combination we have is pitch, roll, surge sway, heave and rotation of pendulum.

To sum up: the motion combination we would perform are:

i. Comb 1: pitch, heave and rotation of pendulum
ii. Comb 2: pitch, roll, heave and rotation of pendulum
iii. Comb 3: pitch, surge, sway, heave and rotation of pendulum
iv. Comb 4: pitch, roll, surge, sway, heave and rotation of pendulum

The reason why yaw motion is always constrained is that: Although the yaw motion has a direct effect on the rotation velocity of pendulum (due to their rotation at the same axis) and cannot be ignored in the real sea state, for the dry tests, taking the yaw motion into account would increase the difficulty of analysis, which is unnecessary. It can be done that considering the effects of coupled yaw motion when analysing the data. The chosen of specific input of motions would take the scale of experimental device and the relationship between different motions, and would be decided in the next chapter.

(b) Spinning Disk

i. Moment of inertia:
The moment of inertia of spinning disk include the mass and diameter of disk. Considering it is impossible for this experiment to change the moment of inertia, it is required that the disk should be replaceable but not necessary to optimum it.

ii. Spinning velocity:
The kinetic energy of spinning disk is a significant parameter for the tests. To simplify the assumption of the experiments, for each set of experiment, disk will accelerate to a certain velocity and remains still for the rest of test. The spinning velocity of the disk should be easily controlled and has a relatively wide and consecutive range for performing, since it's direct solution to increase the energy efficiency.

iii. Position of disk:
Position of disk can also have direct influence on the motions of entire device, however, considering it could be hard for the device to change the position of disk and gravity centre as well, the position of disk is seen as an additional parameter for the experiments. All the specific number of input parameters relative to spinning disk would be discussed in the next chapter.

(c) Moment of inertia of Pendulum:
The moment of inertia of pendulum is also a significant parameter for the energy output. It is affected by the mass of pendulum and the length of pendulum, since there will be a rod-shape component to support the pendulum which can be seen as massless.
Too large or small mass could both result in the low efficiency, since there is a delay between the raise of the wave crest and the raise of the floater bow, which means, the closer natural frequency of floater to the frequency of wave, the higher efficiency the device has [38]. How to choose the moment of inertia of pendulum is also important.

2. Parameters we test:
These parameters are the ones we would test for each set of experiment. It is required that these parameters should be tested with suitable measurement equipment accurately.

(a) Rotation velocity of pendulum:
This parameter is most direct one to see the performance of pendulum by testing its position, velocity and acceleration, which will be greatly helpful for our optimization of system. The rotation performance of pendulum can also be used to compare with the spinning frequency of disk.

(b) Energy output:
If a damper is applied on the rotation, the energy out can be tested. In our experiments, the damping coefficient is not a main parameter we are studying, so we just fix it as a constant. However, it is still meaningful to study the energy output, as it's not proportional to the pendulum rotation, only rotation velocity cannot be enough for analysis. Also, the energy efficiency is one of most important topic we want to study in this research.

The detailed measurement approach would be shown in Section 3.3.4..

3.2. SCALE OF THE EQUIPMENT

3.2.1. FULL SCALE PROTOTYPE

For the Scaled wave energy converter, a scaling factor for entire device is required before fabrication and setup of equipment.
Initially, a possible full scale prototype is analyzed for detailed scaling design of experimental device. The Wello Penguin WEC [39] is taken as our reference shown in Figure

3.4. It has an identical working principle and similar geometry design with our experiments, consisting of a floating hull and a rotating mass inside the hull. The rotating mass is connected to a generator which produces electricity directly into the grid. This product was designed in 2011, and tested in Orkney in 2012 with a grid-connected full-scale prototype. Therefore, the reliability and scalability of this device have been proved, which provides great value to our experiments.

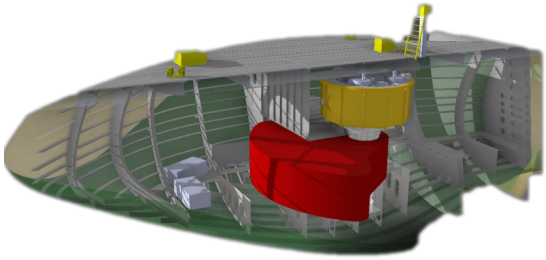

Figure 3.4: Wello Penguin WEC [39]

The scaling of device starts from the geometry. The dimensions of this device are 29 × 16 × 9 (m). Limited by the space of laboratory and requirements of ease of transport, maneuverability and deployment, the device is required to keep around 1 meter scale. Meanwhile, depending on the size of models and tanks used, the model scales are typically of the order of $\frac{1}{30^{th}}$ to $\frac{1}{100^{th}}$ [31]. As the friction losses in the model power take-off should be kept very low fraction ideally, scale of device cannot be very small. Therefore, 1 to 40 is rounded as scaling constant initially, so the dimensions of our prototype can be rounded to 0.8 × 0.4 × 0.3 (m).

3.2.2. SCALING LAW

Generally speaking, there are mainly two ways to scale a WEC: Froude scaling and Reynolds Scaling. People typically use these two non-dimensional quantities to quantify the magnitude of different parameters and they are associated with inertia F_I, gravitation F_I and viscosity F_v

$$F_i \propto \rho U^2 l^2 \tag{3.1}$$

$$F_g \propto \rho g l^3 \tag{3.2}$$

$$F_v \propto \mu U l \tag{3.3}$$

where U is the fluid velocity, g is the gravitational acceleration, l is the length characterising fluid/solid interaction phenomenon and μ is the dynamic viscosity.

$$Fr = \frac{U}{\sqrt{gl}} \propto \frac{F_i}{F_g} \propto \frac{inertial force}{gravitational force} \tag{3.4}$$

$$Re = \frac{Ul}{\sqrt{v}} \propto \frac{F_i}{F_v} \propto \frac{inertial force}{viscous force} \tag{3.5}$$

where υ is the kinematic viscosity ($\upsilon = \mu/\rho$)
Ideally, when designing the scaled model, it is desirable to keep the balance between inertial force, gravitational force and viscous force just as the full scale prototype, requiring the same Froude number and Reynolds number shown in Equation 3.4 and 3.5. However, in practice, this is hard to achieve. In our case, there is no influence of viscous force on body motion and Froude Scaling can be assumed to be satisfied. Let s be the geometric scale between full-scale condition and model. The scaling of different quantities are shown in Table 3.1. The specific process of scaling is provided in Reference [31]. Since the device is affected by the inertia properties and gravity force, the Froude non-dimensional number is used to scale the properties of the device using the geometrical similarity requirement. In this case, the Froude number of the prototype and scaled model should be the same, shown in Equation 3.6. And to simplify it, the scaling factor equals the fraction of the length of prototype and scaled model shown in Equation 3.7

$$Fr_{prototype} = Fr_{scaledmodel} \tag{3.6}$$

$$s = \frac{L_{prototype}}{L_{scaledmodel}} = 40 \tag{3.7}$$

Quantity	Scaling
wave height and length	s
wave period	$s^{0.5}$
wave frequency	$s^{-0.5}$
power density	$s^{2.5}$
linear displacement	s
angular displacement	1
linear velocity	$s^{0.5}$
angular velocity	$s^{-0.5}$
linear acceleration	1
angular acceleration	s^{-1}
mass	s^{3}
force	s^{3}
torque	s^{4}
power	$s^{3.5}$
linear stiffness	s^{2}
angular stiffness	s^{4}
linear damping	$s^{2.5}$
angular damping	$s^{4.5}$

Table 3.1: Froude scaling law for various quantities. s is the geometric scale.

Table 3.1 shows how to scale all the possible parameters. In our experiments, although there is no input from hydrodynamic effect, the scaling of wave height and length in specific area can be considered as the motion input. As a result, the velocity, power and damping torque are the parameters needed to convert to full scale. The term 'power

density' refers to power per unit length.
In this table, s is the geometric scale between model and full-scale conditions. From Equation 3.4, Fr and g are all constant, it is obvious that U scales with $\sqrt{s}$. From the dimension of relationship 3.8

$$[U] = \frac{[L]}{[T]} \tag{3.8}$$

where [U], [L] and [T] are the dimensions of velocity, length and time respectively. So time also scales with $\sqrt{s}$. Take power as example, the dimensions of power are:

$$[P] = \frac{[M][L]^2}{[T]^3} \tag{3.9}$$

Where [M] is the dimension of mass. Since mass if proportional to volume, [M] scales with s^3, therefore, power scales with $s^{3.5}$. Scaling of other factors can also be derived in this way.

3.3. REQUIREMENTS OF COMPONENTS

3.3.1. MOTION PLATFORM

For the conducted research, the simulation of hydrodynamic effects are converted to the direct motion of platform, in this case, the motion platform should be chosen carefully.

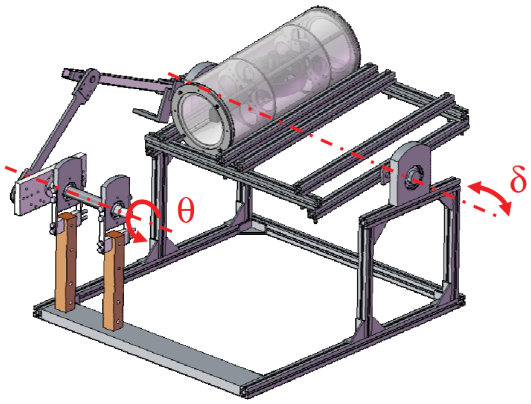

Figure 3.5: Previous work on dry test of wave simulation rig [30]

Figure 3.5 illustrates an axonometry of wave simulation rig, which is mainly composed by an articulated quadrilateral mechanism able to generate a regular sinusoidal motion from a continuous rotation θ given by a motor, and δ results almost in an ideal sinusoid. The amplitude of δ varies from 1.5 to 15 degrees in a step of 1.5 degrees.
From this device, it can be seen that the basic requirements for the platform are that it should be connected to the gyroscopic-pendulum system above closely and perform motions. Additionally, for the motion platform we would use, due to the motion combinations which would be tested, 6 Degree of freedom motion platform is required. And

for each rotation motion, the performance of motion including rotation and translation is required.

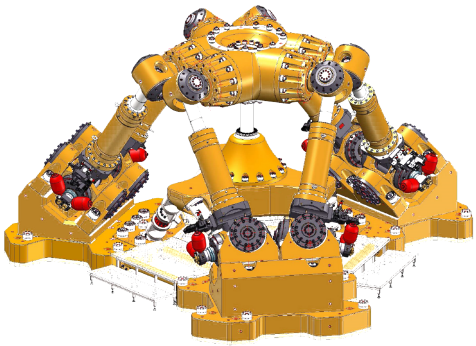

Figure 3.6: TU Delft Hexapod [40]

A 6 DOF motion platform called Hexapod shown in Figure 3.6 is a good reference for us. It can perform rotation ± 5 degrees, and translation ± 150 mm. Although the range does not meet the requirements and the size is too large, we look forward to finding a similar scaled down platform with wider range.
It is important that we can control these motions:

1. The frequency range of the physical waves is 0.15 – 0.28 Hz. To determine the frequency model of the motion platform, the frequency is scaled based on Froude scaling (refer to Table 3.1). In the model, the frequency becomes 0.95 - 1.77 Hz.

2. The rotation angle is calculated based on wave steepness (S = Hs/L). Based on the wave steepness, the required wave angel is in the range 1.94 – 2.02 degree. For the motion platform, the rotation angle can be between 0 – 10 degree.

Parameter	Quantity Range [Unit]
6 Degree of Freedom motions	
Frequency, f	0 – 2.0 [Hz]
Angular angle	0 – 10 [degrees]
Translation	0 – 5 [cm]
Wave Length, L	15.95 – 54.09 [m]

Table 3.2: The motion platform requirements

3. The scale of 1 : 40 is applied in the wave height. The height range of the physical wave is 0.54 – 1.91 m, hence the translation motions can be scaled to 1.35 – 4.78 cm. For the translation motion of the platform (Surge, Sways and Heave), we can have a range between 0 – 5 cm.

To sum it up, the requirements of motion platform are shown in Table 3.2.

3.3.2. GYROSCOPIC-PENDULUM SYSTEM DEVICE

This device should be the "vehicle" for the spinning disk and swinging pendulum, example of Vincent shown in Figure 3.7 from Boren's work. What needs to be aware of is the device shown in Figure 3.7 is a conventional VAPWEC without spinning disk, but the frame of it can provide experience.

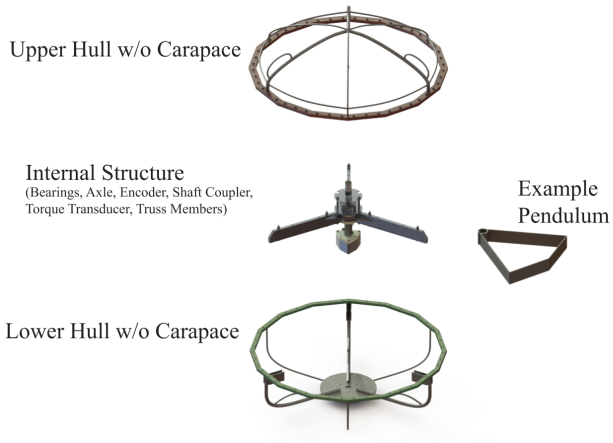

Figure 3.7: CAD model of the generic VAPWEC prototype used in the study [21]

For the energy extraction system including flywheel and pendulum, it must be embedded inside a frame which should be easy to assemble and disassemble. Meanwhile, the need for ease of transport, maneuverability and deployment [21] should be considered as the limiting factors for the final geometry and mass. The frame in Figure 3.7 uses metallic frame structure while the model in Figure 3.5 makes the external shape from an acrylic tube sealed at the end with acrylic caps. Both of the frame materials meet requirements, making the device light and transparent which help us easily observe the motion inside and understand what's happening.

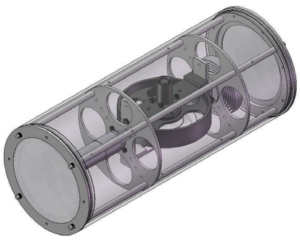

Figure 3.8: ISWEC prototype axonometry [30]

On the other hand, it will be better to make the device watertight for the possible use in

the future. For the internal structure, an example shown in Figure 3.8, the internal structure is embedded in the hull. The internal structure requires consisting of fundamental components including: (i) bearings; (ii) an axle; (iii) a pendulum; (iv) PTO (a rotary encoder, gearbox and brushless motor); (v) a gyro motor; (vi) wire transducer or motion sensor; (vii) load cell
It's required that: These components must be easy to fabricate and also flexible to disassemble. The pendulum and flywheel should be replaceable and the mass of them should be significant compared to the mass of the whole structure. The shape of pendulum is not required, since the factor which matters is the moment of inertia of it.
See Figure 3.8, PTO, gyro and transducer must be mounted on the same axis giving a preferential dimension on the device and the main gyroscopic-pendulum system should be suspended in the middle of the hull, leaving the pendulum rotating freely.
About the dimensions of the gyroscopic pendulum system:

1. The rod length is determined based on natural frequency of the pendulum. If the frequency of range of the real waves is 0.15 – 0.28 Hz, the range of pendulum length can be calculated by using the following formula.

$$\omega = \sqrt{\frac{g}{l}} \tag{3.10}$$

$$2\pi f = \sqrt{\frac{g}{l}} \tag{3.11}$$

$$l = \frac{g}{(2\pi f)^2} = 3.2 - -11.04m \tag{3.12}$$

   The geometry scale of 1:40 is used to scale the pendulum rod. The radius range of the real pendulum is 3.2 – 11.04m. Hence, the scaled model of the pendulum rod length is 8 - 28 cm.

2. Total mass of the real pendulum is assumed 150 MT. Based on the Froude scaling for mass, the pendulum model weight is scaled up to 2.3 kg

3. Motor of the spinning disk that can operate up to 5000 rpm

4. Dimension of the disk should be determined by the numerical model result later. For now, Based on the numerical model, the ideal ratio between the mass moment of inertia of the pendulum model with moment of inertia of the disk model can be fixed as 1 : 12 to have a rough disk mass. For l = 0.25 m, the mass moment inertia of the pendulum model is 0.144 kg.m2, therefore the mass moment of inertia of the disk model is 0.012 kg.m2. The disk dimension will be discussed later in numerical model.

The table 3.3 shows the summary of the required dimensions of gyroscopic pendulum system.

Where Inertial of the pendulum = $m_p * l^2$
Inertia of the disk = ½ * m_d * r^2
The requirements for the measurement equipment will be discussed below separated.

Parameter	Quantity Range [Unit]
Pendulum rod, l	0.08 – 0.28 [m]
Mass of the pendulum model,m_p	2.3 [kg]
Disk motor	0 – 5000 [rpm]
Inertia of the pendulum,I_p	0.016 - 0.196 [kg.m2]
Inertia ratio of the disk model and pendulum	1 : 12
Moment of inertia for the disk model,I_d	0.00133 – 0.0163 [kg.m2]
Disk radius,r	0.0285 – 0.10 [m]
Mass of the disk, m_d	3.26 [kg]

Table 3.3: The gyroscopic pendulum model requirement

3.3.3. AN ELECTRIC MOTOR

A motor with the controlling system is required for driving the disk. Since the spinning velocity is one of parameters we have, the electric motor should be able to accelerate the flywheel to a specific velocity and keep this velocity constant. The torque applied by the electric motor should be tested as well as the acceleration velocity of the disk. Due to the design requirements of the gyroscopic pendulum system, the electric motor embedded inside should be short enough to stay in the structure. Under this circumstance, the possible option is narrowed and the pancake motors will be a reasonable choice shown in Figure 3.9. Research on the market also shows that there exit pancake motors with different diameters and the suitable one will be chosen to adapt the scale of the experiment.

Figure 3.9: Pancake motors [41]

3.3.4. MEASUREMENT EQUIPMENT

1. PTO:
   A PTO (Power Take-Off) system should be applied which converts the mechanical energy into electrical energy [6]. We use it to test the position and velocity of pendulum as well. The PTO used by Bracco is shown in Figure 3.10. It consists of a brushless motor, a rotary encoder and a gearbox. A brushless motor connected with a high efficiency gear will increase the motor shaft speed and decrease the size and weight of the motor, helping it applicable for the tank test.
   The PTO brushless motor should also be controlled in order to apply the damping torque on the gyroscope, and the speed of motor should be controlled constant

large enough.

Figure 3.10: The PTO (motor, gearbox and encoder) [30]

An incremental encoder is equipped inside the PTO for the measurement. It can be applied to measure the position of the pendulum, and meanwhile, the signal received by encoder can be taken the time derivate to evaluate the rotation velocity.
Supply converter for the PTO, motor for gyroscope and the energy storage system should be located off the WEC device and connect with it by cables.

2. Load cell
A load cell equipped with PTO is also required for the measurement of the damping torque on the PTO. While the torque is applied on the load cell, it will create an electrical signal which is coupled directly to torque on it.

Figure 3.11: Load cell [42]

A torque load cell example sees in Figure 3.11, the size and weight of it should be scaled down to adapt to the size of PTO.

3. Wire transducer

A wire transducer located off the motion platform is required to monitor the motions of platform as a backup for the platform control.

3.3.5. DATA ACQUISITION DEVICE

The data acquisition device is required for signal receiving from the transducers including the PTO, load cell and the motion transducer.

3.3.6. CAMERA AND LAPTOP

The camera is required for recording the process of experiments in order to avoid anything left out or forgotten, also as a backup.
The laptop is required for controlling the system including the motor and platform. Also, while doing the experiments, elementary data analysis would help us keep on the right track of research. By the time anything wrong with data analysis is found, we can introspect the problems in experiments immediately

3.4. TEST MATRIX

To have a clear idea on the experimental layout, a couple of test matrices are necessary. The entire list of sets would be listed without specific input number, which will be decided in the next chapter. All of the test matrices are based on the design requirements and the parameters we have.
Since comparison between the energy efficiency of the gyroscopic-pendulum system and the conventional pendulum system is one of our research aims, the first step we consider is dividing the experiments into two groups: one with the disk spinning and the other without, which all have the same motion combinations and pendulum cases. For the spinning disk group shown in Table 3.4, the second column to the forth column show different motion combinations, pendulum cases and disk cases. (the same cases have been omitted in the table)
The motion cases have been discussed above. three pendulum cases mean three different pendulums with different moment of inertia. Besides, we have 9 disk cases for the parameters we have shown in Table 3.6. Therefore, for this group, there are 108 sets of tests to do.

Spinning disk	Motion Comb 1	pendulum case 1	Disk case 1-9
		pendulum case 2	...
		pendulum case 3	...
	Motion Comb 2	...	...
	Motion Comb 3	...	...
	Motion Comb 4	...	...

Table 3.4: Test matrix for the cases of spinning disk

For the group without spinning disk shown in Table 3.5, there is only disk case removed and the other sets remain. Therefore, there are 12 sets to do for this group.

Disk not spinning	Motion Comb 1	pendulum case 1
		pendulum case 2
		pendulum case 3
	Motion Comb 2	...
	Motion Comb 3	...
	Motion Comb 4	...

Table 3.5: Test matrix for the cases of conventional WEC

Disk case	Spinning velocity 1	Spinning velocity 2	Spinning velocity 3
Moment of Inertia 1			
Moment of Inertia 2			
Moment of Inertia 3			

Table 3.6: Table of the disk cases

To sum up, there are 120 sets of tests to do for the research. If the experimental condition allows, more sets of tests could be done.
There are also some limitations of these test matrices, for example, only three cases of each parameter are definitely not enough for the observation of the trend. In this case, we must do some analysis on the parameters we have to find some interesting combinations of parameters we want to study; in another way, to study the sensitivity of each parameter and consider if any parameter is not that important, we can study them later.

4

PRELIMINARY ANALYSIS

In this chapter, a preliminary analysis of numerical model is proposed. Since some rough test matrices have been shown in the last chapter, specific values should be given into the matrices. This chapter will show reasonable analysis approach to narrow the range of parameters which will be proposed for the dry experiment, and find some interesting parameter combinations that might be interesting and should pay attention to in the dry experiments. By the end of this chapter, an improved test matrix will be proposed to specify which values we should test in the simulation and dry experiments for the aim of validation.

4.1. DEFINITION OF PARAMETERS

To analyze the interactions and sensitivity of different parameters, and their effects on the net energy output, it is intuitive to plot the trend of net energy output as figures in terms of different parameters.
However, parameters used in numerical modelling differ with the ones in experimental design, and certain symbols are given to them. Here are listed the parameters we have in the python modeling:

1. The frequency of input motion: $\omega(rad/s)$. Initially, we only input the harmonic pitch motion into the gyroscopic pendulum system, which means we only have one constant frequency of motion. The motion is directly applied on the gyroscopic pendulum system.

2. The rotation amplitude of input motion: A(rad)

3. Moment of inertia of pendulum and disk: I_p and I_d $(kg.m^2)$, shown in Equation 4.1 and 4.2.

$$I_p = m_p l^2 \tag{4.1}$$

$$I_d = \frac{1}{2} m_d r^2 \tag{4.2}$$

Where m_p is the mass of pendulum, l is the length between mass and disk, m_d is the mass of disk, r is the radius of disk.
In the dry experiments, mass and length of pendulum are both worth consideration for the wave energy converter, however, for the convenience in python modelling, we only consider the moment of inertia of pendulum shown in Equation 4.1. In this case, we only change the mass of pendulum to control the I_p.
For the disk, its shape and mass can all be controlled in the dry experiments, so we will not consider the mass and radius separately, but only consider a range of inertia of disk.

4. Inertial ratio: The ratio between moment of inertia of pendulum and moment of inertia of disk: f_I

$$f_I = \frac{I_p}{I_d} \tag{4.3}$$

5. Spinning velocity: The velocity of spinning disk: v(rad/s)

$$1 rad/s = \frac{2\pi}{60} * 1 rpm \tag{4.4}$$

However, while there exist multiple parameters which have varying degrees of impact on the energy output, only studying one at one time seems less meaningful, even though it's given these are independent. Therefore, an overall analysis and individual parameter analysis should all be conducted for the data analysis.

4.2. RANGE OF PARAMETERS

Before studying on the impacts on the net energy output by different parameters, we firstly should define the the range of parameters we use. Although we can study the really wide range of all the parameters in numerical model, it will be meaningless if the range of parameters cannot be applied to the dry experiments.

1. For the definition of input motion(Motion amplitude A and motion frequency ω), the reference wave we are using is shown in Table4.1 which shows the wave profile in real sea state.

Parameter	Quantity Range [Unit]
Water Depth,h	5.39 - 62.10 [m]
Period, T_p	3.60 – 6.54 [s]
Frequency, fp	0.15 – 0.28 [s-1]
Wave Height, H_s	0.54 – 1.91 [m]
Wave Length, L	15.95 – 54.09 [m]

Table 4.1: Reference wave for input motion

The motion angular frequency ω is calculated in Equation4.5.

$$\omega = \frac{2\pi}{T_p} = 2\pi f = 0.96 - 1.74 \tag{4.5}$$

The range of ω is from 0.96 (rad/s) to 1.74 (rad/s). Since we have to scale the wave down as well, which will lead to the increasing of frequency, we choose 0.96(rad/s) as the lower limit of the range. How to scale the frequency is provided in Equation 4.6.

$$[f] = \frac{[1]}{[T]} \tag{4.6}$$

As time scales will $\sqrt{s}$, frequency scales with $\frac{1}{\sqrt{s}}$,(s is scaling factor, chosen as 40 in Section 3.2.2). The angular frequency ranges from 6(rad/s) to 6.32(rad/s) in experimental scale. As the motion platform is required to range from 0 to 2Hz, we can have the range from 0.96(rad/s) to 6.32(rad/s). For the convenience of analysis and discussion, we can round the range to 0.5(rad/s) to 6.5(rad/s)
The motion amplitude ranges from 0 to $\frac{\pi}{4}$(rad), since if the pitch motion exceeds $\frac{\pi}{4}$(rad), the system will obviously become unstable, so the maximum motion is $\frac{\pi}{4}$(rad). Meanwhile, the motion Amplitude is non-dimensional parameter, no need to scale it.

2. The mass, length and inertia of pendulum are all set based on the dimensions of prototype which have been discussed in Section 3.3.2. We keep the length of pendulum constant and only change the mass of pendulum, since the length of pendulum is hard to replace in the dry experiments and only the inertia of pendulum matters for us. The mass of pendulum ranges from $1kg$ to $5kg$, and the inertia of pendulum ranges from $0.078kg.m^2$ to $0.392kg.m^2$. The inertia of disk ranges from $0.005kg.m^2$ to $0.02kg.m^2$ which will be discussed in Section 4.4.2

3. For the angular velocity, it is really uncertain to confirm its range, since it highly related to other parameters like motion frequency and mass of disk. Therefore, as we have other parameters range, we fix other parameters as average values, and plot how the net energy output changes along with angular velocity ranging from 1 to 5000rpm. shown in Figure 4.1. we will narrow the range step by step.

   From Figure 4.1, we can see that, generally, when fixing other parameters and increasing angular velocity from nearly 0 to 5000, the trend of net energy output keeps decreasing really smoothly. Furthermore, the tendency of decreasing is even growing when angular velocity increases(obvious after 1000rpm). In this case, we can narrow the range of angular velocity we study to 0-1000 in Figure 4.2.

   Coming to Figure 4.2, we can see that more noise exists from nearly 0 to 1000, but a fairly clear curve can still be seen. When angular velocity increases from 1 to approximately 350, the net energy output has a slow increase to the peak around 140J, after this, the output has a steep decrease. Concerning that the effects from

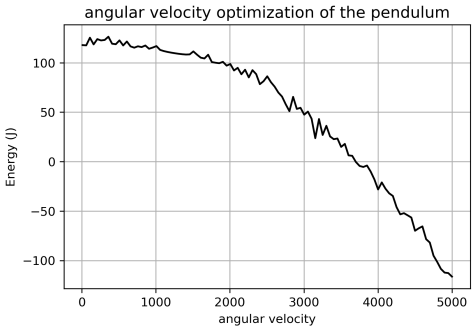

Figure 4.1: Net energy output to disk angular velocity (0-5000rpm)

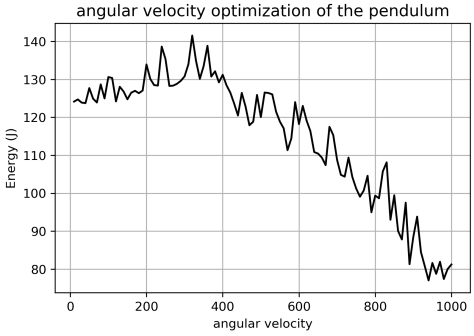

Figure 4.2: Net energy output to disk angular velocity (0-1000rpm)

the change of other parameters may lead to shift of energy peak, we will keep the range of angular velocity from 0 to 1000 for the further research. If necessary, we can also narrow the range to 0 to 500 etc.

The Table 4.2 illustrates the parameter range we will study in the numerical model. The data out of this range will only be used for prediction of trend, but not for the test matrix. And if necessary, the range can also be narrowed.

Parameter	Range [Unit]
Motion frequency, omega	0.5 - 6.5 [/s]
Motion amplitude	0 - $\pi/4$ [rad]
Pendulum rod, l	0.28 [m]
Mass of the pendulum model	1 - 5 [kg]
Angular velocity	0 - 1000 [rpm]
Inertia of the pendulum	0.0784 - 0.392 [$kg.m^2$]
Inertia of the disk	0.005 - 0.025 [$kg.m^2$]

Table 4.2: Range of parameters

A basic combination of parameter case is also necessary for analysis. Since if we want to only analyze one or two parameters, we need to fix other parameters reasonably based on the simulation range. A basic combination of parameter case is chosen in Table 4.3.

Parameter	Quantity [Unit]
Motion frequency, omega	1 [/s]
Motion amplitude	$\pi/4$ [rad]
Pendulum rod, l	0.28 [m]
Mass of the pendulum model	2.5 [kg]
Angular velocity	200 [rpm]
Inertia of the pendulum	0.18 [kg.m^2]
Inertia of the disk	0.01 [kg.m^2]

Table 4.3: Quantity of basic study case

4.3. OVERALL ANALYSIS

In this step, an overall analysis will be done with Buckingham π theorem.
As we have talked in Section 2.5, firstly, we need to combine all the dimensional parameters which are provided at the beginning of this chapter. The motion amplitude A is dimensionless, we just fix it as $\frac{\pi}{4}$, since the maximum rotation amplitude only in one direction will generally generate highest energy output based on the Section 2.3. On the other hand, the change of motion amplitude only changes the amount of output, but will not affect the trend a lot.
Another parameter we cannot forget is that the net energy output should also be included in the π groups as the only dependent variable and the one we study.
Therefore, we have five parameters: E_{net}(J=$kg.m^2/s^2$), I_p($kg.m^2$), I_d($kg.m^2$), v(/s) and ω(/s), and we have three basic dimensions: M(kg), L(m), T(s), Then, we have 5-3=2 π groups including all the parameters. As $E_(net)$ is the only dependent variable, it can only exist in one π group for the convenience of analysis. The process of choosing repeating variables and calculation of π group is skipped in this section, π_1 and π_2 are shown in Equation 4.7 and 4.8.

$$\pi_1 = \frac{\omega * I_p}{v * I_d} \tag{4.7}$$

$$\pi_2 = \frac{E_{net}}{I_d * v^2} \tag{4.8}$$

where E_{net} is the net energy output which equals the energy output (from the pendulum rotation damping) minus the energy input (disk motor etc. excluding the energy into motion platform).
As we can see, for the π_1 group, $\frac{\omega}{v}$ is the fraction between the angular frequency of motion and angular frequency of disk(which is the same as angular velocity). We can set this factor as frequency ratio f_ω shown in Equation 4.9.

$$f_\omega = \frac{\omega}{v} \tag{4.9}$$

The fraction between I_p and I_d is inertia ratio f_I, so π_1 group can be derived into Equation 4.10. We set this as coefficient f.

$$\pi_1 = f_\omega * f_I = f \tag{4.10}$$

Coming to group π_2, the denominator can be seen as the kinetic energy of disk illustrated in Equation 4.11.

$$E_{kinetic} = \frac{1}{2} I_d * v^2 \tag{4.11}$$

Although this $E_{kinetic}$ cannot used to indicate the total energy input into the disk, however, when disk rotating, the inertia and angular velocity of disk don't change, the kinetic energy keeps still during each case, which means, the case with higher kinetic energy will have higher energy input into disk.// So group π_2 can be derived into the the fraction between the net energy output and the disk kinetic energy, we set this as coefficient k shown in Equation 4.12. Literally, if we know k and input energy of disk, we can get the net energy output, so studying on the relationship between k and group π_1 is the point of discussion.

$$\pi_2 = \frac{E_{net}}{2E_{kinetic}} = k \tag{4.12}$$

Although for Buckingham pi theorem itself, the π groups don't have any physical meanings, but it is feasible to use the suitable combination of variables and simplify the equations to find the relationship of each physical component.
In python programming, we make loops for the four independent variables in the range shown in Table 4.2 and plot a scatter chart shown in Figure 4.3. As we focus on the net energy output, we put k at y axis and f at x axis.

Figure 4.3: Pi1 to Pi2 Scatter chart

From Figure4.3, we do qualitative analysis firstly, we can see that:

1. Generally, when f increases (increase of $f_\omega * f_I$), k will increase.

2. For each f, there exists a range of k value.

3. In this figure, it seems that there are two curves, one as the upper limit, the other one as the lower limit, between this two curves all the plotter are contained.

To do a quantitative analysis, we can make a Polynomial Fitting for the scatter chart. The fitting curve is shown in Figure 4.4.

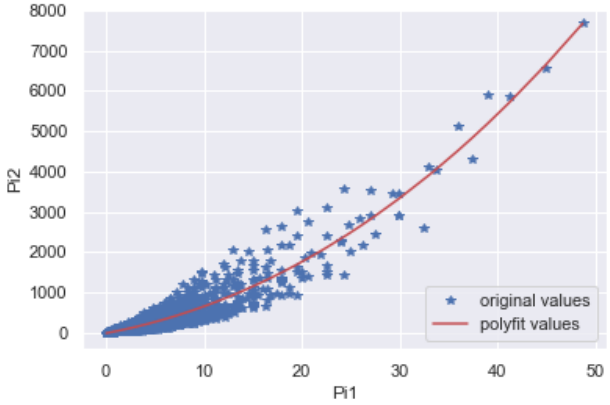

Figure 4.4: Polynomial Fitting of scatter chart

The output polynomial is provided in Equation 4.13, after trying, we will see a cubic fitting is accurate enough for this curve. This is the ratio between net energy output and twice the disk kinetic energy.

$$k = 0.005256 f^3 + 2.056 f^2 - 18.26 \tag{4.13}$$

This figure shows a monotone function for the ratio k, which means we cannot use this figure to narrow the range of parameters in basic case, since the maximum and minimum values exists in both ends. However, this function as well as the trend can be used for the prediction of the net energy output after all the input parameters are confirmed. It is also a part of validation in the dry experiments.

4.4. INDIVIDUAL PARAMETER ANALYSIS

The individual parameter analysis can help us find the sensitivity of each parameter in order to make a correct decision on test matrix design. During this process, some interesting sets of tests can be found while analysis, simulation of them will be done and used to compare with the dry experiments' results.
However, as we have multiple parameters in simulation and intend to study the trend of energy output, only studying one parameter at one time seems too limited. Under this circumstance, heat map is introduced for our analysis.

4.4.1. HEAT MAP

A heat map is a graphical representation of data where some values in matrix are represented as colors. Normally, a 2-D graph can only present two variables in X and y axes, if we want to plot 3 variable in one figure, then 3-D graph is necessary for that. But for a heat map, it can present the values in Z axis by brightness and shade of color in order to include more variables in a 2-D figure.

Take the Figure 4.5 as an example, we can see, on the top left, a heat map shows a bright color at its centre and dark color in the periphery. If we transfer this figure into a counter plot, which is provided in the top right, it shows that the points in the middle have a significant value and the values of z axis will decrease when the point leaves the centre. The same trend is also illustrated in a 3-D graph at bottom right, when x and y =0, it will have a greatest value in z axis.

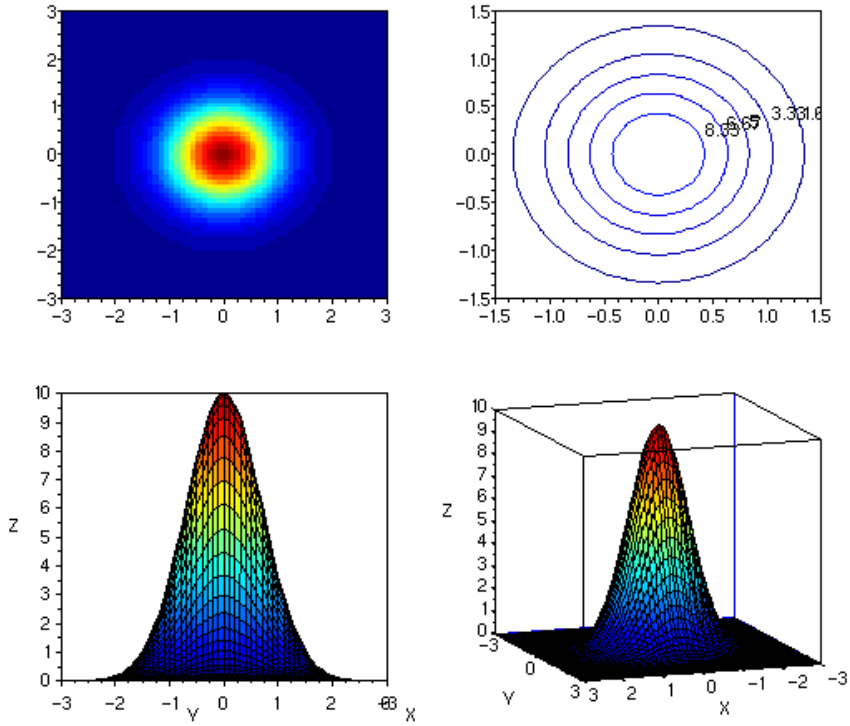

Figure 4.5: Example showing the relationships between a heat map, surface plot, and contour lines of the same data [43]

The figure at bottom right and top left show the same thing, but a heat map is easier to plot than a 3-D one. Also, it is easier to observe as well, since we have to rotate the 3-D figure to see all the values, which cannot be done after printing.

For our heat map, all the values will be marked on the graph for us to observe, because we don't have a lot of points for dry tests, and the display of values help us to record

them.

4.4.2. INERTIAL RATIO

In this system, inertial ratio is a non-dimensional parameter, it shows the relationship between the inertia of pendulum and disk. Since we didn't specify inertia of disk before and the inertia ratio is only factor to specify it, we need to consider it firstly.

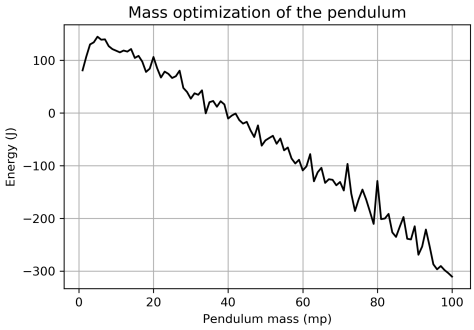

Figure 4.6: Net energy output to mass of pendulum

Shown in Figure 4.6,if we keep the inertial ratio fixed as 20, but only change the moment of inertia of pendulum and disk proportionally, the net energy output will keep changing with the pendulum mass. In this case, it means that even if the ratio between inertial of pendulum and disk keep a constant ratio, this does not give the same energy output. Therefore, we consider the inertial ratio might not be a good parameter on the axis of heat map, fixing it as a reasonable number might be necessary.

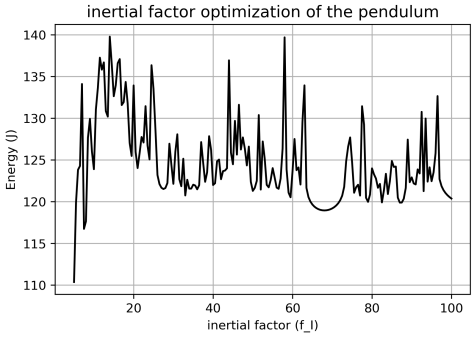

Figure 4.7: Net energy output to inertial factor

what provided in Figure 4.7 is the trend of net energy output in terms of inertial ratio with other factors fixed as base case. In this figure, we can see the general trend of the net energy output, it is obvious that there is a smooth peak around 15 to 20. However, there is also much noise in other range of inertial ratio, so looking for the suitable inertial ratio in this figure seems not very convincing. Therefore, a heat map is used in this

case. As the moment of inertia of pendulum and disk have a closest relationship, we plot these two parameters on one figure which is shown in Figure 4.8. In this heat map, the brightest space locates at the top right where inertial ratio is small and mass of pendulum is large. As a result, a small inertial ratio should be chosen from the figure. We can see that the energy output with inertial ratio less than 20 doesn't differ significantly, we can just choose the inertial ratio = 18 with highest net energy output = 160J when mass of pendulum = 5 kg (f_I=18, m_p = 5,E_{net}=160J). The moment of inertia of disk can also be specified from 0.0044 to 0.022($kg.m^2$), we round it to 0.005 to 0.025($kg.m^2$) in Table 4.2.

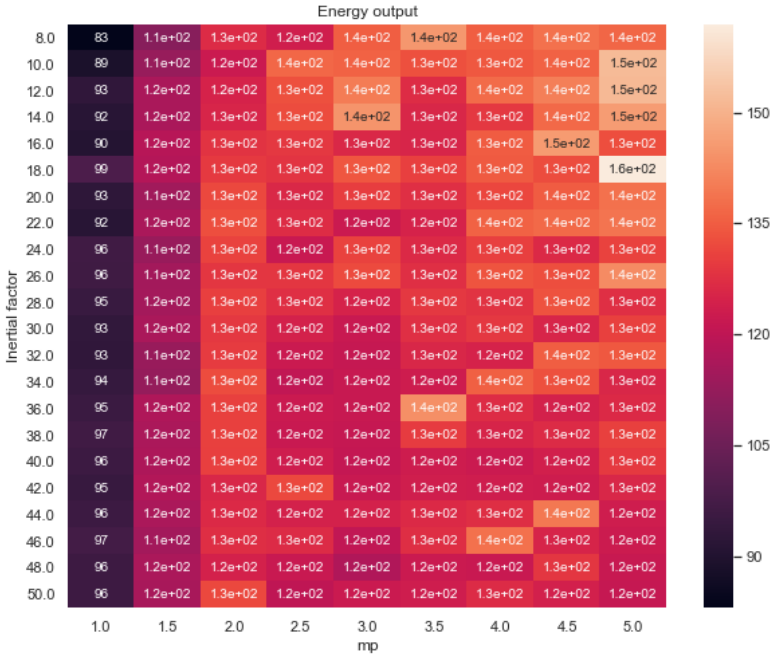

Figure 4.8: Heat map of Net energy output in terms of inertial ratio and moment of inertia

4.4.3. HEAT MAP IN TERMS OF m_p, ω AND V

In this section, we discuss the other parameters' interactions and sensitivity with heat map, in order to improve our test matrix. For example, if one parameter has a great effect on the net energy, then we should have more sets of tests on it. Some combinations of parameters will be tested in our simulation in order to see the performance of pendulum. As we fix the inertial ratio f_I and motion angular amplitude A, the left parameters are m_p, ω and v. As one heat map can display three parameters at one time including net energy

output. We still need three heat maps to show the interactions between the remaining three parameters shown in Figure 4.9, 4.10 and 4.11.

1. The heat map in terms of m_p and ω is shown in Figure 4.9, it is obvious that when frequency increases from 0.5 to 6.5rad/s, the net energy output increases significantly, while the increase of mass can also increase the energy generally but doesn't affect the energy output a lot. It makes sense that higher frequency means higher energy input and higher mass of pendulum means higher energy output on the damper. They all increase the energy output. However, another thing worth discussion is that: at some point, the increase of frequency will lead to decrease of energy output. For example, at m_p = 2.5 kg, when ω=3.5 rad/s, the net energy output is larger than ω= 3 or 4 rad/s. It's really interesting phenomenon which is worth simulation.
   Therefore, from this figure, we will only simulate interesting combinations case 1.1 ($\omega = 3.5 rad/s$, $m_p = 2.5 kg$) and 1.2 ($\omega = 4 rad/s$, $m_p = 2.5 kg$) to study why there is a small peak at $\omega = 3.5 rad/s$. Another one at 1.3 ($\omega = 1 rad/s$, $m_p = 2.5 kg$) can also be tested to see why the pendulum cannot generate energy at low frequency.

2. The heat map in terms of v and ω is shown in Figure 4.10, where the same contributions by frequency can also been seen like the previous one. For each value of frequency, generally when angular velocity increases, the net energy output increases for a short while, followed by a consecutive decrease of energy output. However,for different value of frequency, while the disk angular velocity increases, the peak of net energy output locates at different values of angular velocity. It is also very interesting to see what happen at these peak compare to others.
   Therefore, from this figure, we can see that there is a sudden peak at (v = 950 rpm, ω = 6 rad/s), so we will simulate combinations 2.1($\omega = 6 rad/s$, v = 950rad/s) and 2.2($\omega = 6 rad/s$, v = 900rad/s) to see what happen at this point.

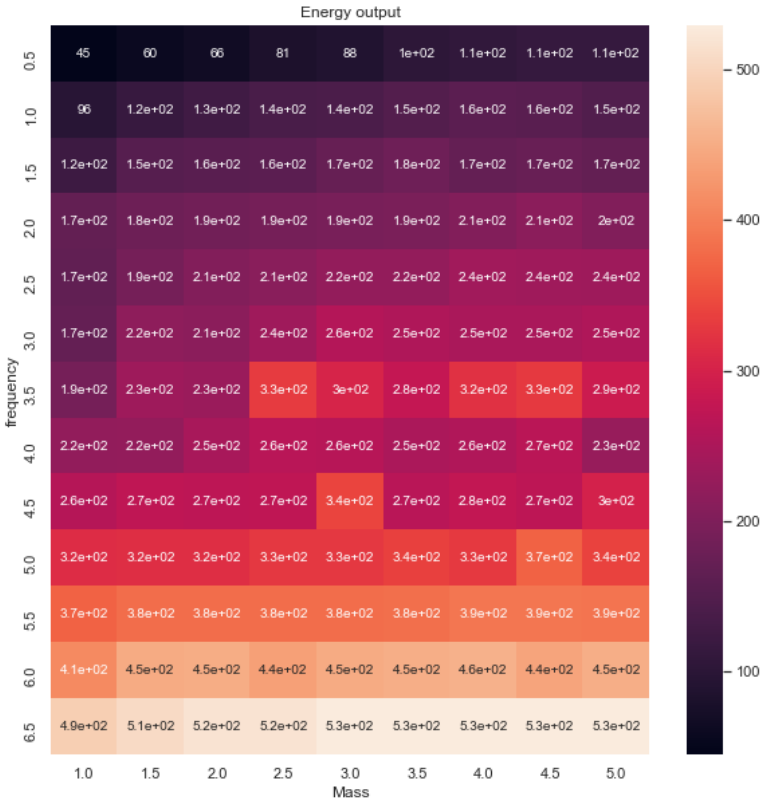

Figure 4.9: Heat map of Net energy output in terms of motion frequency and moment of inertia of pendulum

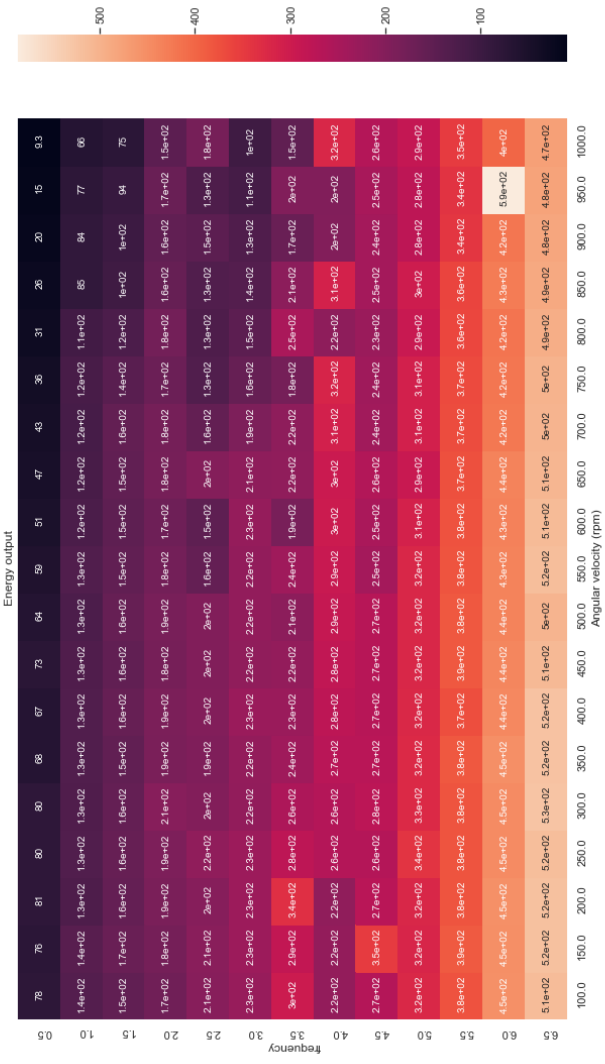

Figure 4.10: Heat map of Net energy output in terms of disk angular velocity and motion frequency

3. The heat map in terms of v and m_p is shown in Figure 4.11. This figure clearly shows that when angular velocity increases, the net energy output has a small increase, and is followed by a continuous decrease after that. As we have simulated this trend in the previous one, we only compare the effect of mass on it. The mass still has a small effect on the energy output, however, we find that at some area, the increase of pendulum mass will result in the decrease of net energy output. That is an interesting condition, because the increase of inertia will definitely increase the energy output, in this case, the increase of mass might change the state of rotation which is worth discussion.
   Therefore, from this figure, we will simulate combinations 3.1($m_p = 5kg$, v = $300rad/s$) and 3.2(m_p = $4.5kg$, v = $300rad/s$) which shows the phenomenon we are interested in.

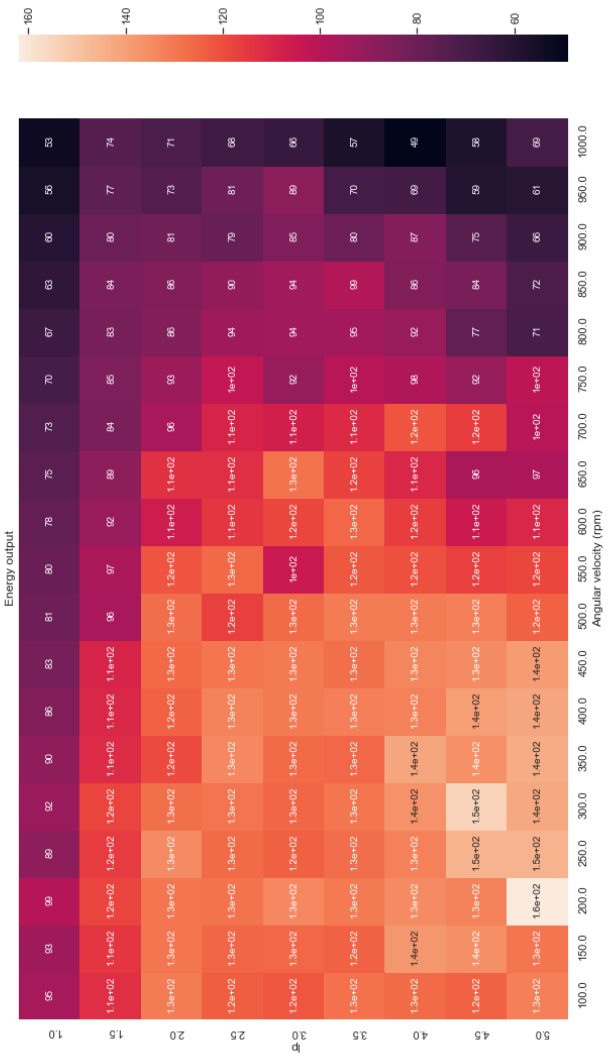

Figure 4.11: Heat map of Net energy output in terms of mass of pendulum and disk angular velocity

After the analysis on the heat map, the interesting combinations of parameters are concluded. The detailed analysis of these cases will be performed in the Chapter 5.

4.5. IMPROVEMENT OF TEST MATRIX

In this section, the test matrix will be improved based on the previous researches. From last section, we can see in our range of parameters, frequency has a highest sensitivity, followed by angular velocity, and the pendulum mass has the least effect on the net energy output. In this case, for the improvement of test matrix, we will have the most sets of tests for motion frequency from 0.5 rad/s to 6.5 rad/s in a step of 0.5 rad/s, then angular velocity from 100rpm to 500rpm in a step of 50rpm. The least sets of pendulum from 1 to 5 kg in a step of 1kg. It is shown in Table 4.4. And 13 × 9 × 5 = 585 in total.

Energy output	motion frequency							
Angular velocity	0.5rad/s	1rad/s	1.5rad/s	....	5.5rad/s	6rad/s	6.5rad/s	Pendulum mass
100rpm								1kg
								2kg
								...
								5kg
150rpm								1-5kg
200rpm								1-5kg
....								1-5kg
400rpm								1-5kg
450rpm								1-5kg
500rpm								1-5kg

Table 4.4: Improvement of test matrix

For comparison with conventional pendulum system without spinning disk, we can have the test matrix with angular velocity = 0 for all cases of frequency and pendulum mass. So there are 13 × 5 =65 in total shown in Table 4.5.

Energy output	motion frequency						
Pendulum mass	0.5rad/s	1rad/s	1.5rad/s	....	5.5rad/s	6rad/s	6.5rad/s
1kg							
2kg							
3kg							
4kg							
5kg							

Table 4.5: Test matrix without spinning disk

In the overall research, we can see that if we want to increase the energy output, we can just try to increase f_I and f_ω. After that, we fix the f_I, the heat maps also gave us the same result, which is increasing the frequency and decreasing the angular velocity will increase the net energy output. To validate this trend, the proposed test matrix will help us while changing different motion frequency and angular velocity in suitable range and step.

	$A(rad)$	$\omega(rad/s)$	$v(rpm)$	m_p(kg)	I_d(kg.$m2$)	f_I
1.1	$\pi/4$	3.5	200	2.5	0.011	18
1.2	$\pi/4$	4	200	2.5	0.011	18
1.3	$\pi/4$	1	200	2.5	0.011	18
2.1	$\pi/4$	6	950	2.5	0.011	18
2.2	$\pi/4$	6	900	2.5	0.011	18
3.1	$\pi/4$	1	300	5	0.022	18
3.2	$\pi/4$	1	300	4.5	0.02	18

Table 4.6: The parameter combinations for simulation

Since we have not done any dry test, it is attractive to us to to observe and analyze the behavior of the system in some cases which have interesting characteristic. So in the simulation chapter, we only simulate the sets we are interested in which are discussed in the previous sections to see the local trend of net energy output by the changes of parameters. The combinations of parameters are provided in Table 4.6.

5

SIMULATION OF TEST MATRIX

In this chapter, the parameter combinations shown in Table 5.1 will be simulated. As mentioned, these cases show some interesting pendulum performances, and they are simulated to see how the pendulum rotation is affected by these parameter changes.

	$A(rad)$	$\omega(rad/s)$	$v(rpm)$	$m_p(kg)$	$I_d(kg.m^2)$	f_I
1.1	$\pi/4$	3.5	200	2.5	0.011	18
1.2	$\pi/4$	4	200	2.5	0.011	18
1.3	$\pi/4$	1	200	2.5	0.011	18
2.1	$\pi/4$	6	950	2.5	0.011	18
2.2	$\pi/4$	6	900	2.5	0.011	18
3.1	$\pi/4$	1	300	5	0.022	18
3.2	$\pi/4$	1	300	4.5	0.02	18

Table 5.1: The parameter combinations for simulation

The simulation results of the cases above output the figures including:

1. Displacement of disk in terms of time
2. velocity of disk in terms of time
3. Displacement of pendulum in terms of time
4. velocity of pendulum in terms of time

and output data including

1. Energy of pendulum output
2. Energy of spinning disk
3. Net energy output

After simulation, Variable-controlling approach is applied to see the effects of certain variable at certain area. The 7 cases have been divided into 3 groups and will be compared with each other to have a general idea on the interesting phenomenon.

a. The simulation results of the cases 1.1 and case 1.2 are shown in Figure 7.1 and 7.2. For the case 1.1:

   - Energy of pendulum output is: 333.6 J
   - Energy input of disk is: 2.5 J
   - Net energy output: 333.2 J

   For the case 1.2:

   - Energy of pendulum output is: 267.1 J
   - Energy input of disk is: 2.3 J
   - Net energy output: 264.8 J

   Comparing the case 1.1 and 1.2, the only difference between these two cases is the motion frequency, where the frequency of case 1.1 is 3.5 rad/s, the frequency of case 1.2 is 4 rad/s, but their pendulum rotation states differ a lot. When we look into the simulation figures of theses two cases, we found that: for the pendulum of 1.1, the pendulum accelerates to a certain value firstly, after that, it starts changing the rotation direction (clockwise and anticlockwise) throughout the whole process from 2 to 10 rad. While for the pendulum of case 1.2, the pendulum always rotates in one direction very smoothly.
   When it comes to the pendulum velocity, we consider that no matter which direction the pendulum rotates, the damper can absorb energy from it, so only the absolute value matters. The pendulum velocity of case 1.1 has a larger range from 0 rad/s to 9 rad/s than the case 1.2 which ranges from 0 to 7.5 rad/s. The reason why case 1.1 has a higher energy output might be because it has a higher average velocity of rotation.

b. The simulation result of the case 1.3 is shown in Figure 7.3

   - Energy of pendulum output is: 139.7 J
   - Energy input of disk is: 2.4 J
   - Net energy output: 137.4 J

   The case 1.3 has a much lower motion frequency than 1.1 and 1.2, it is obviously shown in the Figure 7.3 that the pendulum has few total rotations and the rotation velocity is also low, ranges from 0 - 7 rad/s. From the displacement figure, we can see that the pendulum swings slowly, although the net energy of this case is small, it can be used to study rotation state of pendulum.

c. The simulation results of the cases 2.1 and case 2.2 are shown in Figure 7.4 and 7.5. For the case 2.1:

- Energy of pendulum output is: 635.2 J
- Energy input of disk is: 48.8 J
- Net energy output: 586.5 J

For the case 2.2:

- Energy of pendulum output is: 462.8 J
- Energy input of disk is: 43.9 J
- Net energy output: 418.9 J

The difference between case 2.1 and 2.2 is angular velocity, the case 2.1 shows a small peak around the nearby parameter combinations.
For the displacement of pendulum, the both cases look similar, only case 2.1 changes the direction for once. However, for the pendulum velocity, the case 2.1 ranges from 0 to 13 rad/s, while 2.1 ranges form 4 to 8 rad/s. They have the similar average value, but different range. Therefore, this might be one reason for higher energy output.

d. The simulation results of the cases 3.1 and case 3.2 are shown in Figure 7.6 and 7.7.
For the case 3.1:

- Energy of pendulum output is: 153.2 J
- Energy input of disk is: 10.7 J
- Net energy output: 142.6 J

For the case 3.2:

- Energy of pendulum output is: 164.1 J
- Energy input of disk is: 9.6 J
- Net energy output: 154.5 J

For these two cases, the case 3.2 has a smaller pendulum mass while having a higher energy output than case 3.1.
For the pendulum displacement of these two cases, they all swing slowly and look similar. And also for the velocity, they all range from 0 to 7.5 rad/s, having similar average. However, from the velocity figure, we found that the pendulum velocity of case 3.2 fluctuate quicker than 3.1, which means, it has a higher frequency of changing direction. This might be the reason why it has a higher energy output.

5.1. LIMITATIONS

However, in the simulation period, there are also some limitations of the simulation we need to consider and improve for the dry experiments, including:

1. It doesn't have a high accuracy when predicting the dry experiments. The simulation and analysis can be used to see the effects of different parameters, sensitivity of each parameter and their interactions. But if we want to predict the experiments with higher confidence, we need to include more parameters into the simulation after the equipment are set up. For example, the exact damping coefficient of disk and pendulum, the exact dimensions of floater and energy input on it, etc.

2. The simulation can only explain phenomena superficially without theoretical explanations. To prove whether the interesting phenomenon are real trend or only the random noise, the theoretical proof can be done on this topic.

3. The python modelling can also be improved. While simulation, a problem is found that, the disk velocity fluctuates around a certain level, but we want the velocity keeps still after acceleration. It is because of the coupling effects of the matrix calculations. In this case, the improvement of modelling can be considered.

6

CONCLUSION

For the conclusion of the thesis, the proposed research question is shown below:

- `What are the requirements of the GP device and the experimental setup for the dry test?`

To answer the research question, the conclusions drawn from this thesis can be classified into 4 categories corresponding to the thesis objectives presented in chapter 1, namely:

1. Scaling law of the experiments
2. Components of equipment and requirements of them
3. Parameter analysis and Design of test matrix
4. Preliminary simulation of some interesting sets of experiments

6.1. SCALING LAW

As the experiments will be made in a small scale, the scaling law should be confirmed before it. The Wello Penguin WEC is chosen for our full scale reference, The scaling factor we choose is 1 : 40 based on the consideration of laboratory space. And the dimensions of our prototype are set as $0.8 \times 0.4 \times 0.3$ (m).
The scaling law we choose for the experimental design is Froude Scaling, since gravitational force is one thing which must be considered. After having the scaling law, the scaling for each parameter can also be derived, which is the basis for our requirements of equipment. The capability of equipment should meet the requirements of parameter range we want to test.

6.2. DESIGN OF EXPERIMENTAL EQUIPMENT

The design of experimental equipment includes the definition of all the components of the experimental equipment, and their requirements.
The components of equipment includes:

1. A motion platform; which is used to mimic the hydrodynamic effects and convert them to the direct motions on the floater or gyroscopic-pendulum system.

2. Gyroscopic-pendulum system consisting of spinning disk (with motor) and pendulum; which is the main component of WEC to convert the energy of motion and spinning disk into the pendulum rotation based on the gyroscopic effects.

3. Measurement equipment (sensor, camera and data data acquisition device etc.) which are used to measure the input and output parameters, record the experiments and analyze the output data.

For the motion platform, based on the parameter study on the motion, there are four motion combinations which might be conducted to see the different hydrodynamics effects by different combinations of motions. To meet these requirements, a motion platform which can perform at least 5 motion (pitch, roll, surge, sway, heave and rotation of pendulum) are required. Hexapod is a good example for our requirements.
Considering the real wave profile and scaling factor, the requirements of the frequency and displacement of rotation angle and translation of motion platform are also proposed in the Table 3.2.
For the Gyroscopic-pendulum system, the design of VAPWEC is referred, an external structure and an internal structure are required. The external structure is used to contain all the components and connect with the motion platform which perform the motions on it. The internal structure contains all the main components including: flywheel, pendulum, PTO, motor and other measurement equipment.
Based on the scaling law, the performance range of Gyroscopic-pendulum system is listed in Table 3.3.

6.3. PARAMETER ANALYSIS AND DESIGN OF TEST MATRIX

After designing the experimental equipment, a preliminary test matrix is provided. However, this test matrix contains too many parameters, resulting in too many sets of tests, and we don't have a general idea on each parameters. Then, an parameter analysis is conducted in Chapter 4.
Firstly, the range of all the parameters are constrained based on the design requirements. Then an overall analysis applying Buckingham π theorem to see the trend of net energy output in terms of the combination of all the parameters. A scatter figure of two π groups is provided, and the function of the coefficient k which is ratio between net energy output and twice the disk kinetic energy is fitted.
After that, the individual analysis of parameters is also performed. Heat map is used in this section to analyze the sensitivity and interactions of rest parameters. At the end, final test matrices are provided in Table 4.4 and 4.5.

6.4. PRELIMINARY SIMULATION

In last section, some interesting combinations of parameters are addressed from the analysis. These case are simulated in Chapter 5. After output each case's displacement and velocity of disk in terms of time and displacement and velocity of pendulum in terms

of time, we can study the effect of certain parameter in particular case. This simulation helps us study the isolated cases among the overall trend in order to prepare for the dye experiments.

To sum up, to reach our goal: To propose a dry test setup for the gyroscopic pendulum allowing for systematically investigating the gyroscopic effect on its power output. The design requirements of our device are proposed, and a test matrix of dry experiments are also proposed for set up based on our parameter analysis.

7

RECOMMENDATION

There are also some limitations of this thesis worth further research.

7.1. FURTHER RESEARCH ON EXPERIMENTAL DESIGN

Future work on the experimental design should be done before the experiments, including:

1. Requirements of equipment should be adjusted to the laboratory condition.
   Although the gyroscopic pendulum system will be fabricated by ourselves, the motion platform is still needed to be purchased or borrowed. In this case, the requirements of gyroscopic pendulum system are set as a reference, the dimensions should be adjusted to the size and capability of motion platform.

2. A detailed drawing is necessary in future work.
   For the design of experiments, the requirements of equipment are provided. However, a detailed drawing of all the components including all the connections, materials of components and their detailed dimensions is necessary for fabrication of gyroscopic-pendulum system. In the future work, the suggestion from technician on the design should be obtained in order to make it provide sufficient details for fabrication.

3. The theoretical proof on the parameter study can be provided.
   The parameter study in this thesis is based on the simulation data. It can show the trend of each parameter, but cannon provide the theoretical proof of the trend. For further study, a theoretical derivation should be done on the parameter study

4. The modelling of WEC system can be improved.
   In the simulation Chapter 5, it's found that, because of coupling effect, the disk velocity fluctuate which goes against our assumption on disk velocity. More parameters like disk damping can be included, and coupling effect in the coding should be solved for the future research.

APPENDIX I

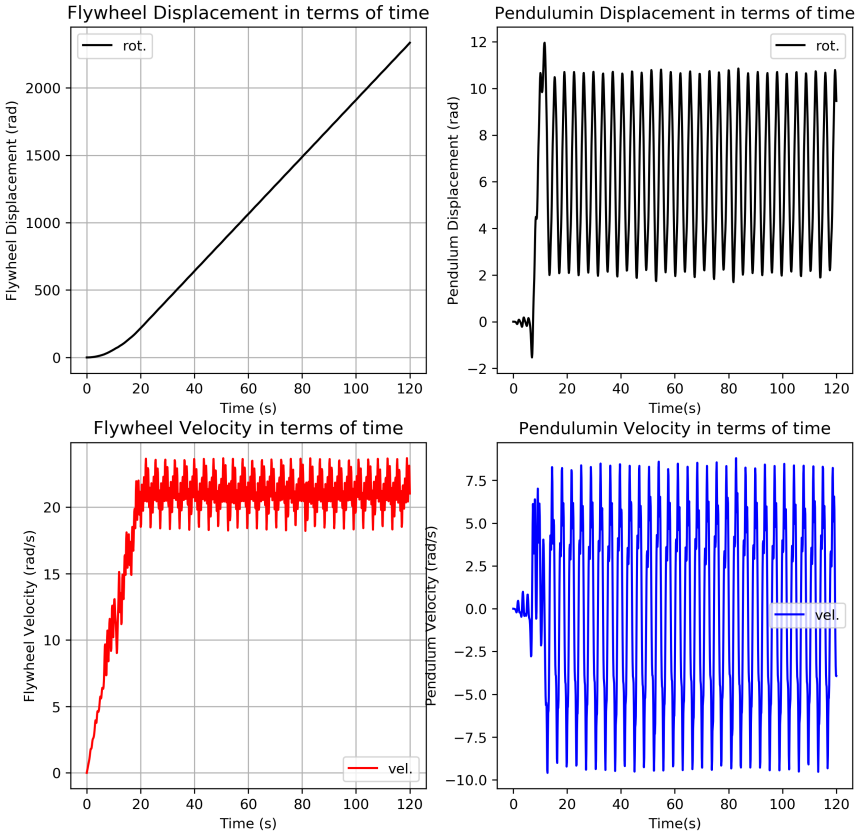

Figure 7.1: Simulation plot of case 1.1

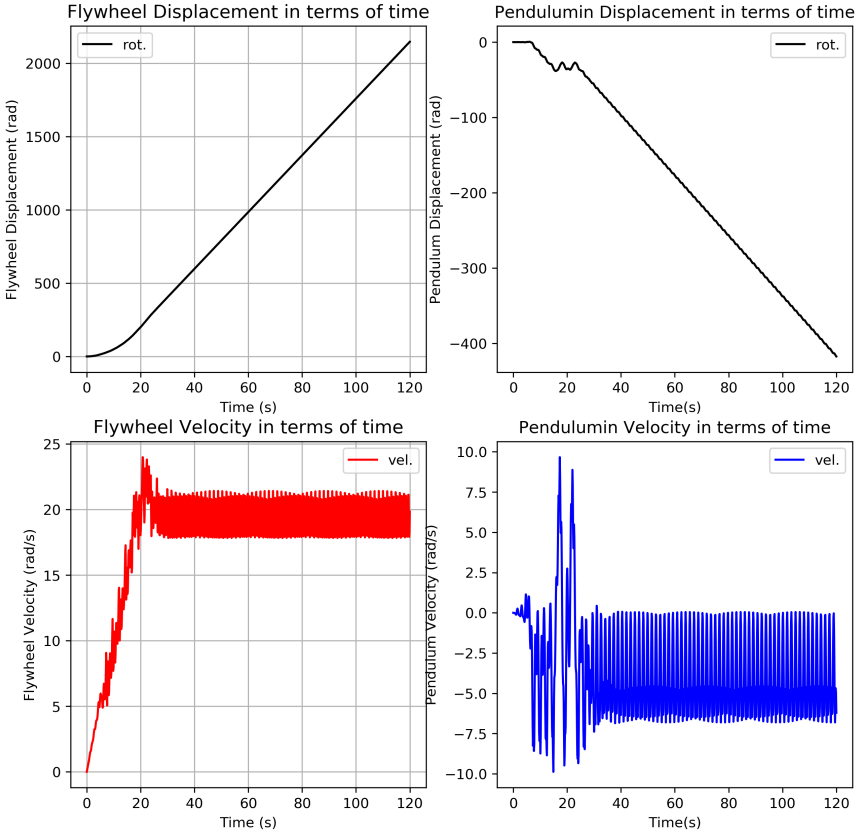

Figure 7.2: Simulation plot of case 1.2

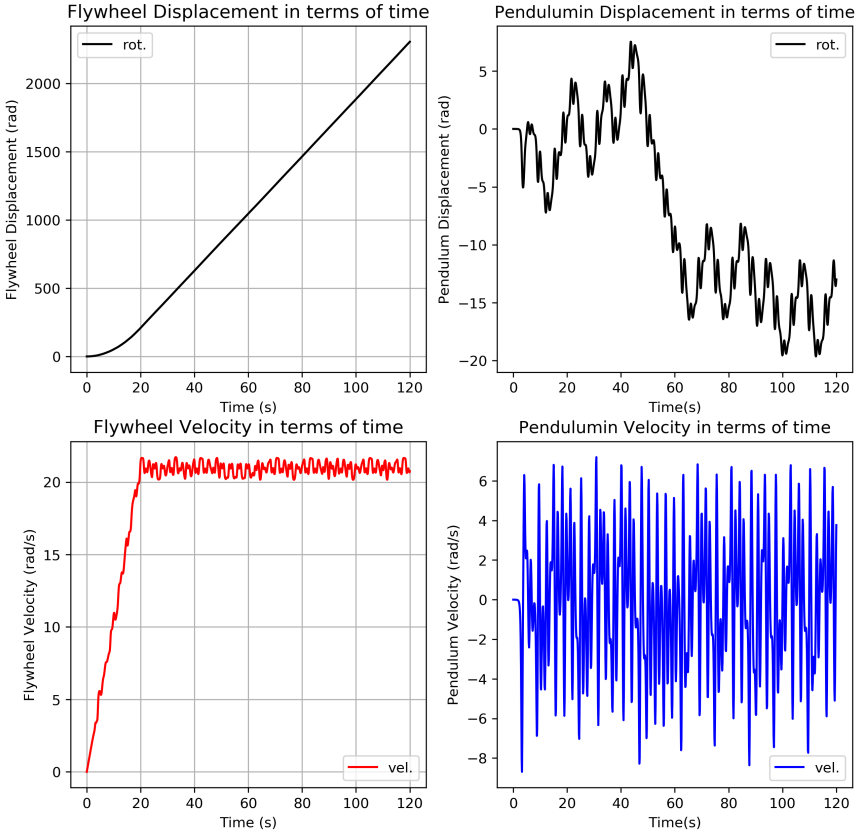

Figure 7.3: Simulation plot of case 1.3

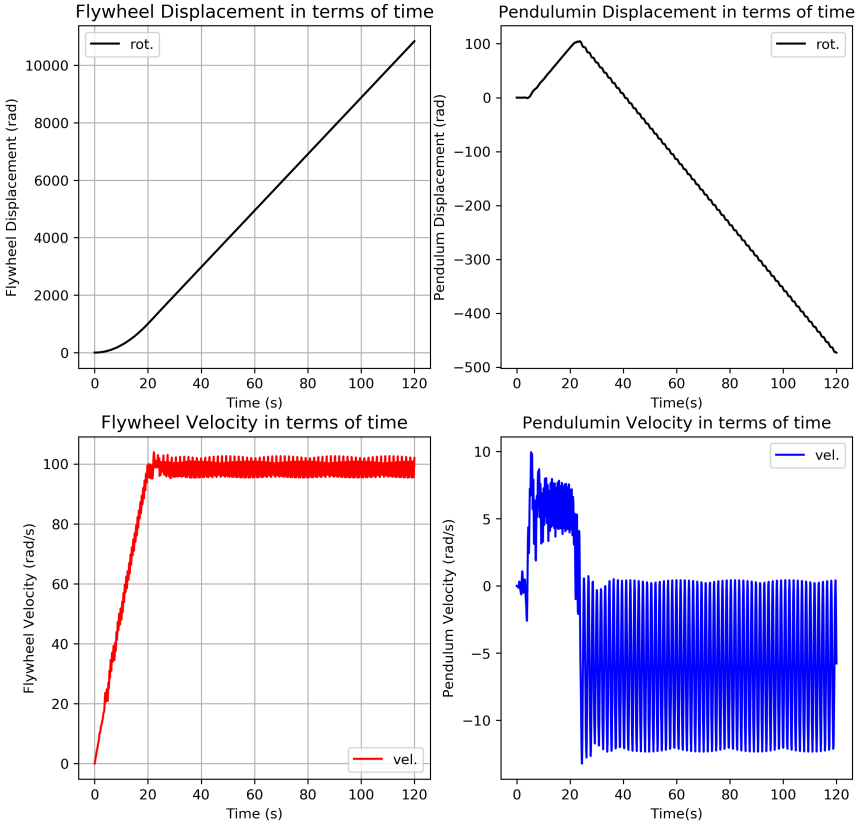

Figure 7.4: Simulation plot of case 2.1

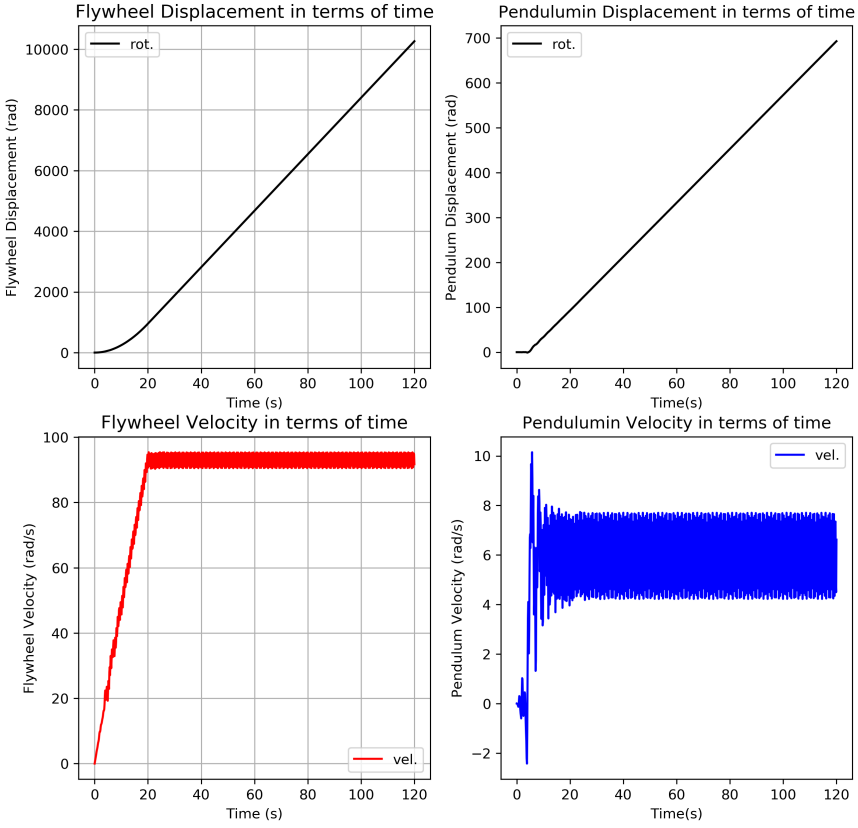

Figure 7.5: Simulation plot of case 2.2

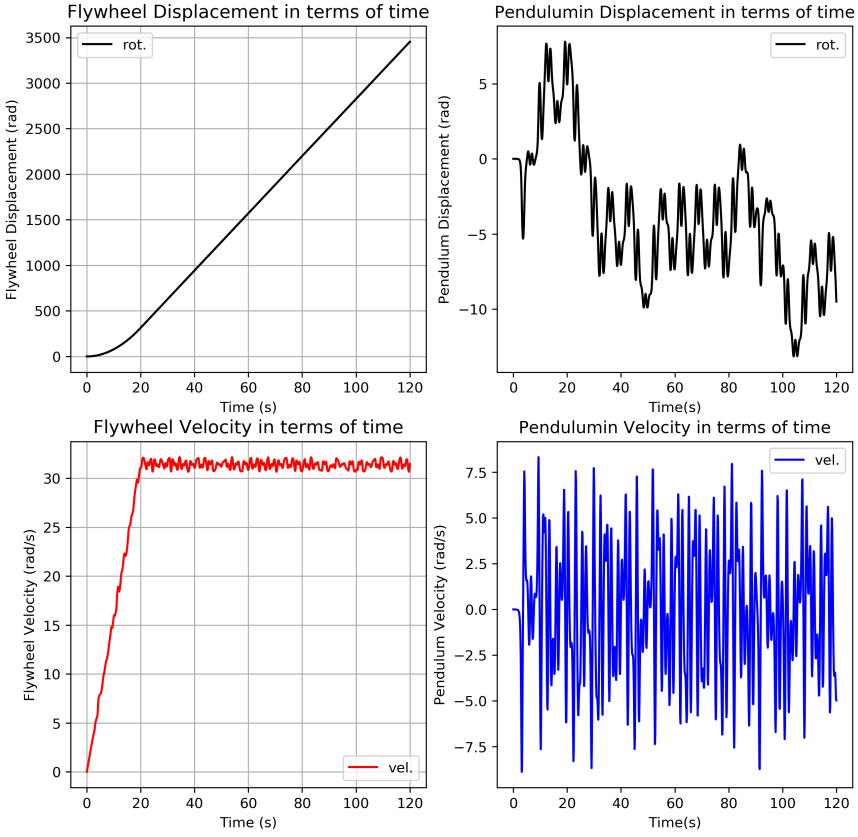

Figure 7.6: Simulation plot of case 3.1

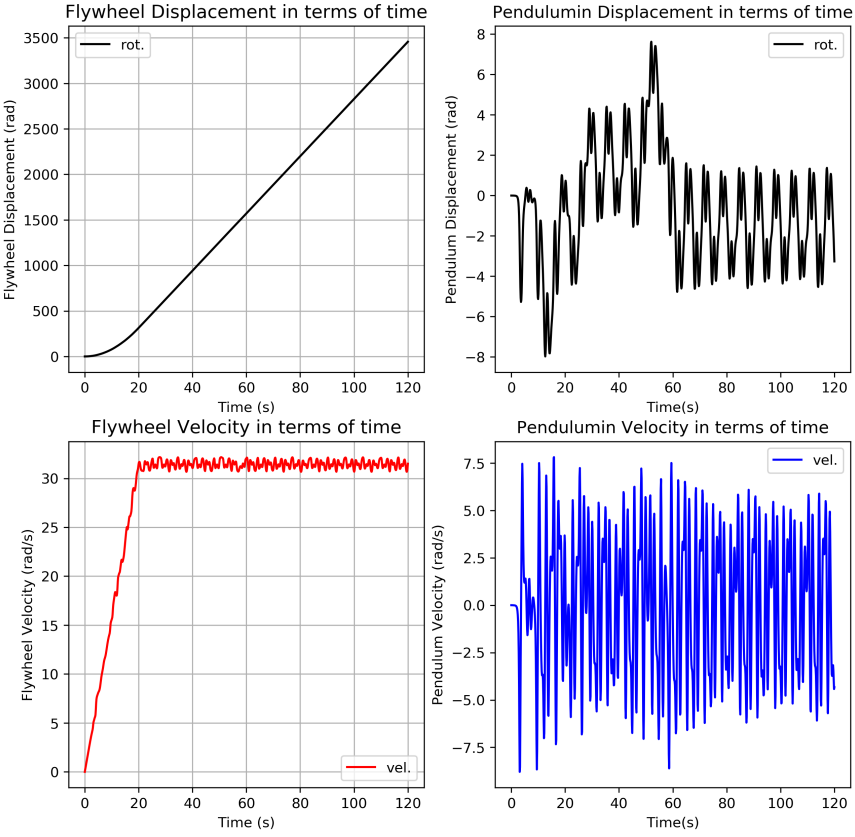

Figure 7.7: Simulation plot of case 3.2

REFERENCES

[1] Todor Todorčević, Pavol Bauer, Jan Abraham Ferreira, and Rick van Kessel. A modulation strategy for wide voltage output in dab based dc-dc modular multilevel converter. In *IECON 2014-40th Annual Conference of the IEEE Industrial Electronics Society*, pages 4514–4520. IEEE, 2014.

[2] John Callaghan and Richard Boud. Future marine energy. results of the marine energy challenge: Cost competitiveness and growth of wave and tidal stream energy. *Carbon trust*, 2006.

[3] Joao Cruz. *Ocean wave energy: current status and future prespectives*. Springer Science & Business Media, 2007.

[4] Blake C Boren. Vertical axis pendulum wave energy converters: investigating control strategies and the deployment of a scaled generic prototype. 2015.

[5] Stephen H Salter. Wave power. *Nature*, 249(5459):720–724, 1974.

[6] Alessandro Battezzato, Giovanni Bracco, Ermanno Giorcelli, and Giuliana Mattiazzo. Performance assessment of a 2 dof gyroscopic wave energy converter. *Journal of Theoretical and Applied Mechanics*, 53(1):195–207, 2015.

[7] Benjamin Drew, Andrew R Plummer, and M Necip Sahinkaya. A review of wave energy converter technology, 2009.

[8] Herbert K Sachs and George A Sachs. Mechanism for generating power from wave motion on a body of water, September 28 1982. US Patent 4,352,023.

[9] Iii Ernest C Hinck. Wave power generator, January 25 1966. US Patent 3,231,749.

[10] Johannes Falnes. *Ocean waves and oscillating systems: linear interactions including wave-energy extraction*. Cambridge university press, 2002.

[11] DV Evans. Power from water waves. *Annual review of Fluid mechanics*, 13(1):157–187, 1981.

[12] Diana Bull and Margaret E Ochs. Technological cost-reduction pathways for attenuator wave energy converters in the marine hydrokinetic environment, 2013.

[13] JKH Shek, DE Macpherson, and MA Mueller. Power conversion for wave energy applications. 2010.

[14] David J Pizer, Chris Retzler, Ross M Henderson, Fiona L Cowieson, Martin G Shaw, Beth Dickens, and Rosalind Hart. Pelamis wec—recent advances in the numerical and experimental modelling programme. In *Proceedings of 6th European wave tidal energy conference*, pages 373–378, 2005.

[15] Ingvald Straume. File:wave energy concepts overview numbered.png. https://en.wikipedia.org/wiki/File:Wave_energy_concepts_overview_numbered.png, 2010.

[16] Eduard Muljadi and Yi-Hsiang Yu. Review of marine hydrokinetic power generation and power plant. *Electric Power Components and Systems*, 43(12):1422–1433, 2015.

[17] Tethys. Capturing energy from waves with a point absorber buoy, surface attenuator, oscillating water column, or overtopping device. https://tethys.pnnl.gov/technology-type/wave, 2019.

[18] Aquamarine Power. How oyster wave power works,. http://www.aquamarinepower.com/technology/how-oyster-wave-power-works/, 2011.

[19] F. Gardner. Archimedes wave swing. http://www.teamwork.nl/en/portfolio/project/archimedes-wave-swing, January 2008.

[20] JRM Taylor, M Rea, and DJ Rogers. The edinburgh curved tank. In *5th European Wave Energy Conference, Cork, Ireland*, pages 307–314, 2003.

[21] Blake C Boren, Pedro Lomonaco, Belinda A Batten, and Robert K Paasch. Design, development, and testing of a scaled vertical axis pendulum wave energy converter. *IEEE Transactions on Sustainable Energy*, 8(1):155–163, 2017.

[22] Blake C Boren. On the modeling and control of horizontal pendulum wave energy converters. 2013.

[23] Ted KA Brekken, Ken Rhinefrank, Annette von Jouanne, Alphonse Schacher, Joseph Prudell, and Erik Hammagren. Scaled development of a novel wave energy converter including numerical analysis and high-resolution tank testing. *Proceedings of the IEEE*, 101(4):866–875, 2013.

[24] Singiresu S Rao and Fook Fah Yap. *Mechanical vibrations*, volume 4. Prentice hall Upper Saddle River, 2011.

[25] S Graham Kelly. *Schaum's Outline of Mechanical Vibrations*. McGraw-Hill Companies, 1996.

[26] G Bracco, E Giorcelli, and G Mattiazzo. Experimental testing on a one degree of freedom wave energy converter conceived for the mediterranean sea. *TMM 2008*, 2008.

[27] Giovanni Bracco, Ermanno Giorcelli, and Giuliana Mattiazzo. One degree of freedom gyroscopic mechanism for wave energy converters. In *ASME 2008 International Design Engineering Technical Conferences and Computers and Information in Engineering Conference*, pages 895–902. American Society of Mechanical Engineers, 2008.

[28] Don Glassman. Italian linear defy to the waves. *Popular Mechanics Magazine*, 55 (4):626–634, 1931.

[29] G Bracco, E Giorcelli, G Mattiazzo, M Pastorelli, and J Taylor. Iswec: design of a prototype model with gyroscope. In *2009 International Conference on Clean Electrical Power*, pages 57–63. IEEE, 2009.

[30] G Bracco. Iswec: a gyroscopic wave energy converter [ph. d. thesis]. *Publications Open Repository Torino*, 2010.

[31] Gregory Payne. Guidance for the experimental tank testing of wave energy converters. *SuperGen Marine*, 2008.

[32] Giovanni Bracco, Ermanno Giorcelli, Giuliana Mattiazzo, Vincenzo Orlando, and Mattia Raffero. Hardware-in-the-loop test rig for the iswec wave energy system. *Mechatronics*, 25:11–17, 2015.

[33] Sergej A Sirigu, Giacomo Vissio, Giovanni Bracco, Ermanno Giorcelli, Biagio Passione, Mattia Raffero, and Giuliana Mattiazzo. Iswec design tool. *International Journal of Marine Energy*, 15:201–213, 2016.

[34] Giovanni Bracco, Andrea Cagninei, Ermanno Giorcelli, Giuliana Mattiazzo, Davide Poggi, and Mattia Raffero. Experimental validation of the iswec wave to pto model. *Ocean Engineering*, 120:40–51, 2016.

[35] Lurohman M. Masturi. Gyroscopically enhanced vertical axis pendulum for wave energy conversion. *EWTEC 13th Conference proceeding, 2019 in Napoli Italy*, 2019.

[36] Jh Bertrand. Sur l'homogénéité dans les formules de physique. *Cahiers de recherche de l'Academie de Sciences*, 86:916–920, 1878.

[37] Lord Rayleigh Sec. R.S. Viii. on the question of the stability of the flow of fluids. *The London, Edinburgh, and Dublin Philosophical Magazine and Journal of Science*, 34 (206):59–70, 1892. doi: 10.1080/14786449208620167. URL https://doi.org/10.1080/14786449208620167.

[38] Nicola Pozzi, Giovanni Bracco, Biagio Passione, Sergej Antonello Sirigu, and Giuliana Mattiazzo. Pewec: Experimental validation of wave to pto numerical model. *Ocean Engineering*, 167:114–129, 2018.

[39] Wello. Penguin wec. http://www.wello.eu/penguin.php, 2014.

[40] TUDelft. 3me hexapod. https://www.tudelft.nl/en/3me/departments/maritime-and-transport-technology/research/ship-and-offshore-structures/facilities/hexapod/, 2019.

[41] Medital. Printed motor works pancake motors. https://www.medital.com/products/printed-motors-workspancake-motors, 2019.

[42] Forsentek. Torque load cell torque sensors measure torque. http://www.forsensor.com/sale-8832677-torque-load-cell-torque-sensors-measure-torque.html, 2019.

[43] wikipedia. Heat map. https://en.wikipedia.org/wiki/Heat_map, 2019.